

Composite strongly interacting dark matter

James M. Cline, Zuowei Liu, and Guy D. Moore

Department of Physics, McGill University, 3600 Rue University, Montréal, Québec, Canada H3A 2T8

Wei Xue

INFN, Sezione di Trieste, SISSA, via Bonomea 265, 34136 Trieste, Italy

It has been suggested that cold dark matter (CDM) has difficulties in explaining tentative evidence for noncuspy halo profiles in small galaxies, and the low velocity dispersions observed in the largest Milky Way satellites (“too big to fail” problem). Strongly self-interacting dark matter has been noted as a robust solution to these problems. The elastic cross sections required are much larger than predicted by generic CDM models, but could naturally be of the right size if dark matter is composite. We explore in a general way the constraints on models where strongly interacting CDM is in the form of dark “atoms” or “molecules,” or bound states of a confining gauge interaction (“hadrons”). These constraints include considerations of relic density, direct detection, big bang nucleosynthesis, the cosmic microwave background, and LHC data.

I. INTRODUCTION

Cold dark matter (CDM) has proven in most respects to be an excellent description of the 22% of the universe’s energy density that is not baryonic nor dark energy. There are however a few suggested problems in its ability to predict some of the observed properties of dark matter halos. These are the behavior of the density profile near galactic centers, which comes out too cuspy in N -body simulations [1–4], as well as the overabundance of prominent satellite galaxies, relative to observations: the “too big to fail” (TBTF) problem [5, 6]. Long ago it was pointed out that strong elastic scattering of dark matter with itself, with cross section per mass $\sigma/m \sim 0.1 - 1 \text{ cm}^2/\text{g}$,¹ would ameliorate the first of these problems [7, 8]. More recent work has shown that the TBTF problem can also be addressed in this way (see ref. [9] for a review).²

The idea of strongly interacting dark matter (SIDM) fell out of favor in light of subsequent arguments that σ/m should be less than $0.02 \text{ cm}^2/\text{g}$ to avoid making observed elliptical halos become too spherical [11]. A similar but weaker upper limit of $0.7 \text{ cm}^2/\text{g}$ was found using simulations of the Bullet Cluster [12]. The arguments leading to the more stringent bound have recently been reexamined [13] in light of improved simulations, leading the authors to conclude that the halo ellipticity bound should be relaxed to the level of $0.1 \text{ cm}^2/\text{g}$. The same authors argue that this value is moreover consistent with what is needed to solve the problems of halo cuspiness and excess substructure [14]. Subsequently ref. [15] studied this issue using a higher resolution simulation and concluded that a larger value of $0.6 \text{ cm}^2/\text{g} = 1.1 \text{ b}/\text{GeV}$

is needed to produce the cores inferred in dwarf galaxies by ref. [16].³ We adopt this figure in the following for the preferred value of the SIDM cross section.⁴

To appreciate the challenge of achieving such a large cross section if dark matter is a fundamental particle, consider scalar DM with a quartic interaction $(\lambda/4!)S^4$. The cross section over mass is given by $\sigma/m = \lambda^2/(128\pi)(m/\text{GeV})^{-3} \cdot 4 \times 10^{-4} \text{ b}/\text{GeV}$. Even at the largest sensible value of $\lambda \sim 32\pi^2/3$, where the one-loop correction to σ becomes of the same order as the tree level cross section, to reach the level of $\sigma/m = 0.1 \text{ cm}^2/\text{g}$ requires a small dark matter mass, $m \sim 400 \text{ MeV}$, introducing a new hierarchy problem worse than that of the weak scale. It is possible to overcome this limitation in a more complicated model where heavy dark matter interacts with itself via a light vector boson, with mass $m_V \lesssim 1 - 100 \text{ MeV}$ [18]–[27]. But here the question of naturalness has just been transferred to the vector boson mass scale (except in the limit where it is massless [28]).

On the other hand, normal atoms and nuclei in the visible sector have σ/m close to or above the values of interest. The large cross section of atoms arises because they themselves are large, due to being weakly bound. For nuclei the cross section is large because of the residual strong interactions, mediated by relatively light mesonic or nuclear bound states. It is therefore interesting to consider dark analogues of these kinds of states in a hidden sector as candidates for dark matter. Models of atomic dark matter have been previously considered (although starting from different motivations) in

¹ This is related to the alternate unit of cross section per mass $1 \text{ b}/\text{GeV} = 0.56 \text{ cm}^2/\text{g}$, where $\text{b} = 10^{-28} \text{ m}^2$. We take $c = 1$ throughout.

² A recent paper [10] finds that the TBTF problem is ameliorated by updating the values of cosmological parameters that go into the simulations.

³ Ref. [17] shows that different assumptions about the parametrization of the dwarf halos than made in [16] can significantly reduce the evidence for cores in these systems, though not disprove their existence.

⁴ This value of σ/m may start to be in marginal conflict from halo ellipticity bounds, which limits $\sigma/m < 1 \text{ cm}^2/\text{g}$ [13]. More detailed investigations using numerical simulations of halo shapes for intermediate values of σ/m will be needed to settle the question.

refs. [29]–[37].⁵ Historically, the first atomic dark matter model was in the context of mirror symmetry, in which the dark sector is an exact copy of the visible one (see refs. [43]–[44] for a review). We do not consider this scenario here, since we will show that the dark electron is always much heavier than m_e in the models that give the desired self-interaction cross sections. The case in which mirror symmetry is broken [45] might at first seem to offer a greater possibility to provide a concrete realization of this scenario, but we will show in section II that it is also incompatible with our criteria.

Composite (“hadronic”) dark matter models involving confining gauge forces have been considered in refs. [46]–[68], with much of the recent motivation stemming from observations of DAMA [69] and other direct detection experiments, or the idea of linking dark matter genesis to baryogenesis and thus explaining their similar abundances. (Indeed a common attribute of atomic and “baryonic” DM models is that they are asymmetric, with the relic abundance arising analogously to the baryon asymmetry rather than by thermal freeze-out.) Here we add to the previously considered motivations by emphasizing the natural capacity of composite dark matter for having strong enough self-interactions to overcome the halo structure problems.

The main particle physics alternative to SIDM for addressing the shortcomings of CDM has been warm dark matter (WDM), with mass of order keV; see ref. [70] for a recent review.⁶ Ref. [9] argues that warm dark matter of a given mass is not able to solve the halo structure problems while remaining consistent with Lyman- α determinations of the power of density fluctuations on small scales [72]–[74]. The latter place a lower limit of at least 4 keV on the dark matter mass, which is too large to allow for effective smoothing of central cusps of galactic halos. It should be noted however that this conclusion depends upon the assumed value of the Milky Way halo mass M_{halo} ; if $M_{\text{halo}} > 1.4 \times 10^{12} M_{\odot}$, then lower WDM masses can be tolerated [75].

In section II we outline the requirements of atomic DM models to have a strong enough self-interaction cross section. Here we also treat the possibility that the dark matter is primarily in molecular form, finding a larger region of viability to be SIDM. We discuss constraints from direct detection and cosmology on the atomic models. In section III we turn to the possibility of dark “mesons” in a strongly coupled dark sector, showing that they can be SIDM if sufficiently light (30–100 MeV). To get the right

relic density by thermal production, we argue that the hidden quarks should interact with massless dark photons that kinetically mix with the normal photon, and we demonstrate an explicit model, discussing the cosmological constraints that apply. The case of hidden sector “baryons” as the dark matter is examined in section IV, and that of glueballs in section V. We summarize our results in section VI.

II. ATOMIC DARK MATTER

We first examine the simplest example of atomic dark matter [29], a bound state of elementary particles transforming under a hidden $U(1)'$ symmetry with charge g' . The constituents are the dark “proton” \mathbf{p} and “electron” \mathbf{e} , assumed to be spin-1/2 particles. The analogues of the fine structure constant and Bohr radius are $\alpha' = g'^2/4\pi$ and $a'_0 = (\alpha'\mu_{\mathbf{H}})^{-1}$ respectively, where $\mu_{\mathbf{H}} = m_{\mathbf{e}}m_{\mathbf{p}}/(m_{\mathbf{e}} + m_{\mathbf{p}})$ is the reduced mass. Taking account of binding energy $E_b \cong \alpha'^2\mu_{\mathbf{H}}/2$, the mass of the ground state dark atom is $m_{\mathbf{H}} = m_{\mathbf{p}} + m_{\mathbf{e}} - E_b$. We will also introduce the mass ratio $R \equiv m_{\mathbf{p}}/m_{\mathbf{e}}$, which should be treated as a model parameter. It enters in the scattering cross section through the combination

$$\frac{m_{\mathbf{H}}}{\mu_{\mathbf{H}}} \cong R + 2 + R^{-1} \equiv f(R) \quad (1)$$

where we have ignored the binding energy contribution to $m_{\mathbf{H}}$. It has been shown in [29, 34] that as long as α' is sufficiently large ($\gtrsim 10^{-2}$, as we will verify for most of the relevant parameter space), the ionized fraction of the atoms is suppressed, and dissipative processes that would lead to collapse of the halo and formation of dark stars are negligible. Thus dark halos will not differ radically relative to expectations for CDM. Only those more subtle properties that we want to alter will be affected by the strong elastic self-interactions.

II.1. Dark atoms

For simplicity we will initially assume that dark atoms do not form a significant population of molecules, but we will come back to this question below. We thus consider the elastic cross section for dark atom scattering, which we have studied in detail in a previous paper [37]. In that work we computed both the elastic and momentum transfer cross sections as a function of energy, over a large range of $R \sim 1 - 3000$, noting that the dependence upon R can be very strong due to divergences of the scattering length in the channel where the electrons are in the spin-singlet state. The origin of these divergences can be understood from the form of the Schrödinger equation when rewritten using atomic units of distance ($a'_0 = 1$) and energy ($\epsilon_0 \equiv \alpha'^2\mu_{\mathbf{H}} = 1$):

$$\left(\partial_r^2 - \frac{\ell(\ell+1)}{r^2} + f(R)(E - V_{s,t}) \right) u_{\ell}^{s,t}(r) = 0 \quad (2)$$

⁵ We do not consider the scenario of ${}^4\text{He } X^{--}$ bound states of ref. [38] since exotic stable X^{--} particles appear to be ruled out by big bang nucleosynthesis constraints [39], which are far stronger for charge-2 relics than the usually studied charge-1 relics [40], and by anomalous hydrogen constraints [41]. For directly detecting such bound state dark matter, see e.g. [42].

⁶ Ref. [71] recently proposed that ultra-light axions comprising 85% of the total dark matter could provide an alternative solution to the problems of CDM.

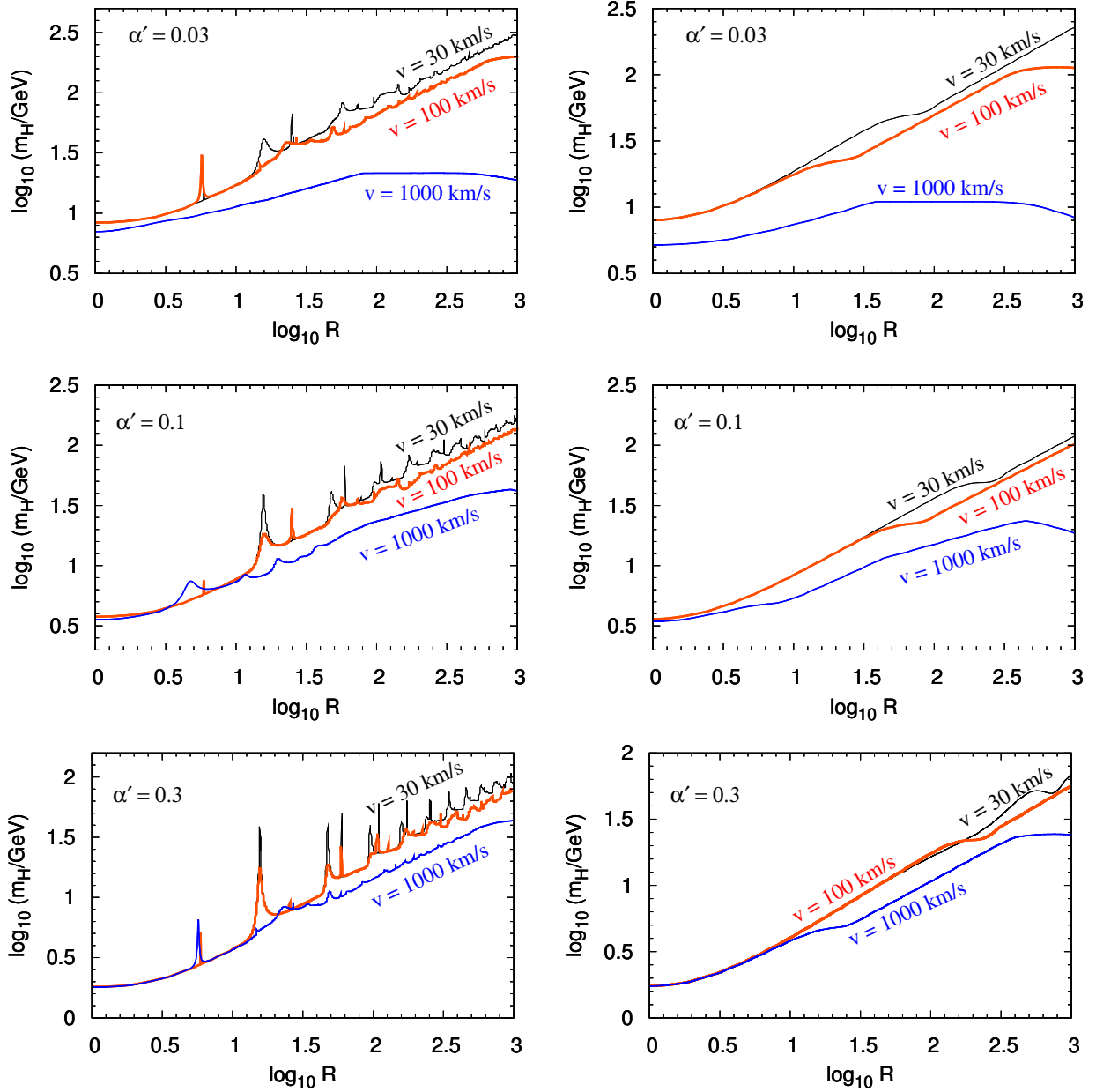


Figure 1. Left: contours of constant $\sigma/m_{\mathbf{H}} = 0.6 \text{ cm}^2/\text{g}$ in the plane of $m_{\mathbf{H}}$ and $R = m_{\mathbf{p}}/m_{\mathbf{e}}$ (using the atom-atom momentum transfer cross section) at center of mass energies $E = m_{\mathbf{H}}v^2$, for $v = 30, 100$ and 1000 km/s . Top to bottom plots are for $\alpha' = 0.03, 0.1$ and 0.3 respectively. Right: analogous contours for molecular \mathbf{H}_2 scattering, with $\sigma/(2m_{\mathbf{H}}) = 0.6 \text{ cm}^2/\text{g}$ and $E = (2m_{\mathbf{H}})v^2$, but still using $m_{\mathbf{H}}$ for the vertical axis.

Here $u = r\psi$ and the subscripts s, t label the spin-singlet and triplet contributions to the scattering. The singlet potential V_s is much deeper than the triplet one V_t , and it rapidly acquires more bound states as R is increased since the potential is multiplied by $f(R) \sim R$. Each time a bound state energy approaches zero, the scattering length diverges. From fig. 2 of ref. [37], it can be seen that at low velocities, the singlet channel typically dominates the scattering, except at values of R (such as in the real world) where the singlet scattering length happens to be

close to zero.

Using the methods described in ref. [37], we have identified the regions of atomic dark matter parameter space for which the momentum transfer cross section has the fiducial value $\sigma/m_{\mathbf{H}} = 0.6 \text{ cm}^2/\text{g}$. The results are displayed as a function of $m_{\mathbf{H}}$ and R for several values of α' (0.03, 0.1, 0.3) in the left-hand plots of fig. 1. We do not consider smaller α' since, as noted in [37], then the ionization fraction starts to become large in parts of the parameter space and the atomic description is no longer

appropriate. We display contours of constant $\sigma/m_{\mathbf{H}}$ for several DM velocities, $v = 30, 100, 1000$ km/s, appropriate for dwarfs, Milky-Way-like galaxies and galactic clusters, respectively. Because the cross sections can have significant velocity dependence, these curves do not generally coincide, although there are ranges of parameters where they do so, namely for R not too large and α' not too small.

To better understand the results of fig. 1, we recall from ref. [37] that a typical scattering cross section for dark atoms is of order $100 a_0'^2$; therefore $\sigma/m_{\mathbf{H}} \sim 100 \alpha'^{-2} f^2(R) m_{\mathbf{H}}^{-3}$, implying that

$$\frac{m_{\mathbf{H}}}{\text{GeV}} \cong \left(\frac{R}{5.3 \alpha'} \right)^{2/3} \quad (3)$$

for $R \gg 1$. At fixed values of R and α' , the higher curves in fig. 1 require larger $m_{\mathbf{H}}$ to have the same cross section; therefore if $m_{\mathbf{H}}$ was also held fixed the lower curves would represent smaller values of σ . DM distributions at the largest scales—clusters of galaxies—which have the highest velocity dispersion, thus have the smallest σ , except in the regions of large α' and small R where the curves overlap. Where the curves do not overlap, the cross section is generally largest for the smallest velocities, but there are exceptions corresponding to resonances, which give rise to the spiky structure as a function of R . In particular, we find that the bumps at $R \cong 5.6$ are due to a p -wave resonance in the singlet channel (and thus do not appear in the scattering length), similar examples of which are prominent in fig. 4 of [37].

Mirror symmetry, in which the dark sector is an exact copy of the standard model, provides an explicit realization of atomic dark matter, but one that is not compatible with the SIDM constraint (3), which requires that $m_{\mathbf{H}} = 1.3$ TeV for the SM values $R = 1836$, $\alpha' = 1/137$. Extra freedom is possible in the version of the model in which mirror symmetry is spontaneously broken. In this case the values $m_{\mathbf{H}} \cong 5$ GeV and $m_{\mathbf{e}} \cong 50$ MeV have been promoted in a scenario where the visible and dark baryon asymmetries are linked [45]. However (3) then requires $\alpha' \sim 1$, far from the value of $1/137$ that is still predicted despite mirror symmetry breaking.

II.2. Molecular dark matter

In the interstellar medium, hydrogen gas exists not only in atomic form, but also in H_2 molecules, whose abundance is significant especially in cold or dusty regions where ionizing radiation is less present. Although H_2 is subject to destruction by ionizing radiation due to its relatively weak binding energy of 4.5 eV, it nevertheless requires ionized constituents such as p or H^- for its formation, since the processes involving charged particles, such as $p + \text{H} \rightarrow \text{H}_2^+$ followed by $\text{H}_2^+ + \text{H} \rightarrow \text{H}_2 + p$, are much more efficient for producing H_2 than the direct (but much slower) process $\text{H} + \text{H} \rightarrow \text{H}_2 + \gamma$. Therefore the relative abundance of molecules and atoms is

not simple to predict. Nevertheless (as we argued in [37]) it seems plausible that molecules could be prevalent in a dark sector where there are no stars, hence no ionizing radiation, since there is still a small ionized fraction of the dark atomic constituents, of order $f_i \sim 10^{-10} \alpha'^{-4} R^{-1} (m_{\mathbf{H}}/\text{GeV})^2$, that can give rise to the catalyzed production of H_2 . A quantitative prediction of the H_2 abundance is beyond the scope of this paper. Instead we consider the prospects for dark molecules to have the desired self-interaction cross section, assuming they constitute the dominant dark matter component.

The scattering cross sections of dark molecules were computed in ref. [37]. Using the methodology described there, we determined the analogous constraints, from imposing that $\sigma/m = 0.6 \text{ cm}^2/\text{g}$, to those of dark atoms and display them in the right-hand plots of fig. 1. The general behavior of the curves is similar to their atomic counterparts in fig. 1, but the molecular ones are smoother as a function of R , due to the shallow potential for molecule-molecule scattering, which does not develop any bound state until $R \sim 700$. Moreover, as also shown in ref. [37], the scattering length for molecules has a zero near $R = 280$, which gives rise to the pronounced dip in the cross section at $v = 10$ km/s and $\alpha = 0.1$. This is a qualitative difference with respect to the atomic case, where σ at $v = 10$ km/s is almost always larger than at $v = 100$ km/s.

II.3. Direct detection constraints

The model as presented so far does not give rise to any signal in DM detectors, but by the simple addition of a kinetic mixing term $\frac{1}{2} \epsilon F^{\mu\nu} F'_{\mu\nu}$ between the photon and the dark $\text{U}(1)$ gauge boson, it does so, as was pointed out in ref. [32]. In that case the dark electron \mathbf{e} and proton \mathbf{p} acquire millicharges $\mp e\epsilon$ under $\text{U}(1)_{\text{em}}$, and so can scatter on protons by exchange of a photon. Even though the dark atom is electrically neutral, as long as $R \gg 1$ the charge cloud of \mathbf{e} does not overlap strongly with that of \mathbf{p} and so \mathbf{H} will scatter on protons electromagnetically, just like a normal H atom except for the reduced charge of the dark constituents. In the case of $R = 1$, there is strong cancellation between the two charge clouds and the Coulomb scattering amplitude vanishes in the first Born approximation. We will consider this special case separately.

For $R \gg 1$, ref. [32] showed that the cross section for atomic DM scattering on protons is $\sigma_p = 4\pi(\alpha\epsilon\mu_{p\mathbf{H}})^2 a_0'^4$ where $\mu_{p\mathbf{H}}$ is the reduced mass of the $p\text{-}\mathbf{H}$ system. In the present context, we can fix the value of a_0 for a given $m_{\mathbf{H}}$ by assuming that the relationship between $m_{\mathbf{H}}$ and R shown in fig. 1 is satisfied, for given choices of α' and DM velocity. Then $a_0 = f(R)/(\alpha' m_{\mathbf{H}})$. We choose $v = 10$ km/s since this tends to give the largest self-interaction cross section. The maximum value of ϵ allowed by LUX [76] can be found by setting the predicted σ_p equal to the LUX limit, relaxed by the factor $(A/Z)^2 = (131.3/54)^2$

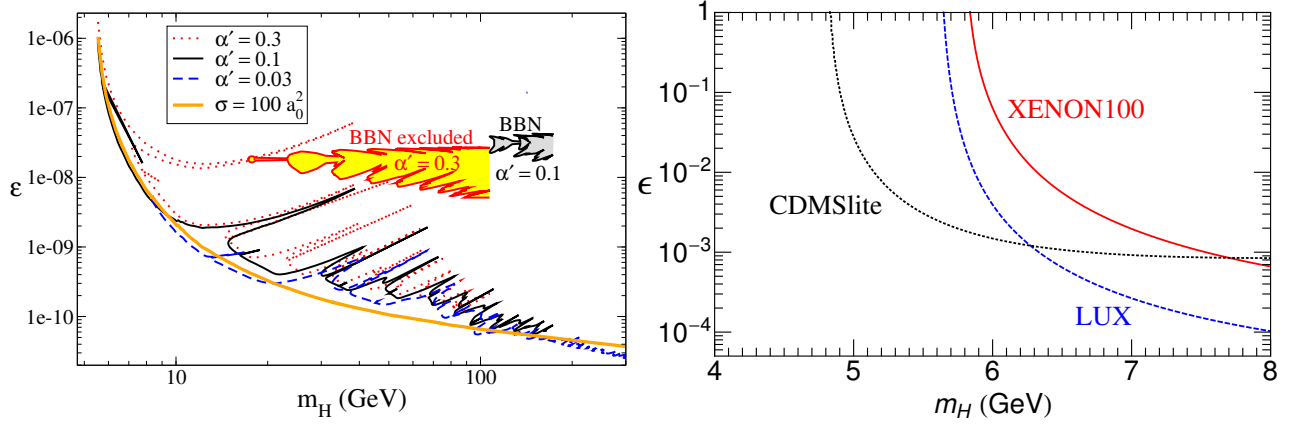


Figure 2. Left: upper limits on kinetic mixing in millicharged DM model from LUX [76] bounds, assuming the relation between $m_{\mathbf{H}}$ and R for atomic DM with $v = 30$ km/s in fig. 1 is satisfied, for each value of $\alpha' = 0.03, 0.1, 0.3$. Also shown is the limit obtained from approximating the self-interaction cross section as $\sigma = 100 a_0^2$. The shaded regions for indicated values of α' are ruled out by big bang nucleosynthesis constraints, as described in section II.4. Right: constraints on ϵ for the special case $R = 1$, in which the interaction of atomic DM with visible matter is through an inelastic magnetic moment transition. The DM mass splitting is determined by the relationship (4) that produces the target value of the self-interaction cross section.

due to the coupling only to protons. In fact, the relation between $m_{\mathbf{H}}$ and R can be double-valued due to the resonant peaks in σ , so we scan in R to produce parametrized limit curves in the plane of ϵ and $m_{\mathbf{H}}$. These are shown in fig. 2(left). Except for the positions of the resonances, the α' dependence in these curves is weak. For comparison we show the result of the rough approximation for the self-interaction cross section of $\sigma = 100 a_0^2$, which results in the relation $a_0 = 5.3 m_{\mathbf{H}}^{1/2} \text{ GeV}^{-3/2}$, which works well at low $m_{\mathbf{H}}$ (apart from resonances), but gives somewhat too low a prediction of σ at higher $m_{\mathbf{H}}$.

In sect. II.4 we will show that a small interval of $\epsilon\sqrt{\alpha'}$ is excluded over some range of dark electron masses, (depending upon assumptions about initial conditions after reheating) to avoid overpopulating the dark photons during big bang nucleosynthesis (BBN). The excluded regions (shaded) in the $m_{\mathbf{H}}-\epsilon$ plane are shown in fig. 2(left), assuming that m_e is determined by $m_{\mathbf{H}}$ and α' so as to give the desired self-interaction cross section. For large values of $\alpha' \gtrsim 0.3$, this intersects part of the parameter space of interest for direct detection, but for smaller α' there is no overlap between the BBN-excluded regions and those which can be probed by direct searches.

In the case of $R = 1$, the leading interactions of dark atoms are, for sufficiently small α' , the magnetic inelastic scatterings that change the total spin of the atom. These were studied in detail in ref. [33], with attention to the region $m_{\mathbf{H}} \sim 9 - 12$ GeV as suggested by excess events from the CoGeNT experiment [77]. For strongly interacting atomic DM satisfying $\sigma/m_{\mathbf{H}} = 0.6 \text{ cm}^2/\text{g}$, we find that $m_{\mathbf{H}}$ and α' are related by

$$m_{\mathbf{H}} = 0.8 \alpha'^{-2/3} \text{ GeV} \quad (4)$$

so that $m_{\mathbf{H}}$ ranges between 1.8 and 8.3 GeV for $\alpha' = 0.3 - 0.03$. The rate of nuclear scatterings is sensitive to

the mass difference $\delta m_{\mathbf{H}}$ between the lowest DM state and the hyperfine excitation where the relative spins of the proton and electron are reversed, $\delta m_{\mathbf{H}} = \alpha'^4 m_{\mathbf{H}}/6$, from which we can eliminate α' in favor of $m_{\mathbf{H}}$ using (4), for the case of self-interacting DM.

In fig. 2(right) we show the constraints on the kinetic mixing for the $R = 1$ model from CDMSlite [78], XENON100 [79] and LUX [76], for models that satisfy (4) and therefore have the required self-interaction cross section.⁷ The mass splitting $\delta m_{\mathbf{H}}$ ranges from 14 to 1 keV for $m_{\mathbf{H}} = (5 - 8)$ GeV. The constraints on ϵ are much weaker than in the case of $R \gg 1$ due to the inelastic magnetic dipole versus elastic Coulomb nature of the interaction. We do not show the CoGeNT-allowed region on fig. 2 because we find that the assumption (4) needed to have strongly-interacting DM is contrary to getting a good fit to the CoGeNT excess events. If we nevertheless impose (4), the best fit region is at higher masses than allowed for strongly interacting atomic dark

⁷ The XENON100 limit is computed as described in appendix D of [33]. For the LUX limit, the number of events is computed using the acceptance function given in fig. 9 of [76] (black '+' symbols). The 90% upper limit on the events due to DM, $N < 2.4$ events, is used for low mass DM. Following LUX, the events below 3 keVnr are not included. For CDMSlite, which has not made its data publicly available, we randomly distributed events within histogram bins in the energy range 841 eVnr (nuclear recoil threshold) to 4 keVnr (avoiding the activation line near 5.3 keVnr). For low mass DM the exclusion limit is essentially controlled by the low recoil energy spectrum, so the 90% limits are computed using the p_{Max} method [80] in the nuclear recoil energy range [0.841, 4] keVnr. Although for elastic DM, the CDMSlite limits extends to much lower DM mass range, the limits for millicharged atomic dark matter terminate near $m_{\mathbf{H}} = 5$ GeV due to inelasticity.

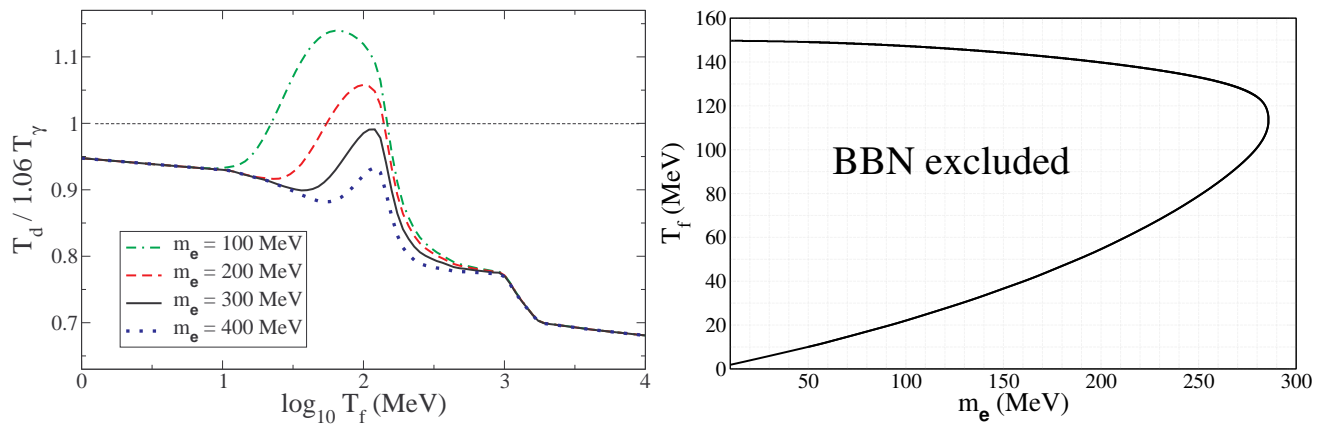


Figure 3. Left: Dark to visible temperature ratio divided by the limiting value 1.06, as determined by eq. 5, as a function of the freeze-out temperature T_f for the process $\gamma'e \leftrightarrow \gamma e$. Relation is shown for several values of m_e . Right: the resulting excluded region (shaded) in the m_e - T_f plane.

matter with small ionization fraction, with the edge of the 99.7% C.L. region just reaching the right-hand side of the plot. There is essentially no overlap between the CoGeNT events and the SIDM parameter space within this model.

II.4. Big bang nucleosynthesis constraints

The atomic DM model can potentially provide an excess of radiation during the epoch of big bang nucleosynthesis (BBN). This provides stringent constraints on mirror dark matter [81]–[82] since both the dark photons and dark electrons/neutrinos can contribute to the excess. In our case, m_e is always greater than 100 MeV so that only the dark photons can contribute (and we do not consider dark neutrinos). Taking the 95% c.l. limit on the effective number of extra neutrino species $\delta N_\nu < 1.44$ [83], the dark photon temperature T_d at the time of BBN is constrained to be $T_d/T = (\frac{7}{8}\delta N_\nu)^{1/4} < 1.06$ relative to that of the visible photons. If there is no interaction between the dark and visible sectors, then the excess in dark radiation depends upon initial conditions, and can be compatible with the constraints if reheating into the dark sector after inflation is less efficient than into the visible one.

An interesting scenario is that where gauge kinetic mixing between the dark and visible photons provides an interaction between the two sectors, causing the dark proton and electron to have millicharges ϵe under electromagnetism. This can lead to equilibration between the dark and visible photons through scattering on dark electrons, $\gamma'e \leftrightarrow \gamma e$. At low temperatures, the interaction rate is governed by the Thomson cross section $\sigma = (8\pi/3)\alpha\alpha'(\epsilon/m_e)^2$, but for $T > m_e$ one must perform the thermal average of the Compton cross section as described in appendix A. This interaction can come into equilibrium at temperatures above $\sim m_e$ if $\sqrt{\alpha'}\epsilon$ does not fall below a critical value that we find to be given by

$(\sqrt{\alpha'}\epsilon)_c \sim 10^{-10.6}(m_e/\text{MeV})^{0.57}$, assuming that $T_d = T$. It goes back out of equilibrium at lower temperatures as the dark electrons disappear from the bath.

Although it is beyond the scope of this paper to make a detailed study of the thermal history of the dark sector, it seems reasonable to suppose that $T_d = T$ at some early time, if ϵ is not too small. For example, even if the dark sector was initially much colder than the visible one, say at the moment of reheating, the interaction $\gamma\gamma \rightarrow e^+e^-$ comes into equilibrium by $T \sim m_e$ if $\alpha\epsilon \gtrsim (m_e/M_p)$. We will be interested in $m_e \sim 100$ MeV, for which this implies $\epsilon \gtrsim 10^{-8}$, compatible with the magnitude for which we will find BBN constraints. For the following discussion, we assume that $T_d = T$ at temperatures of a few GeV as an initial condition.

Under these assumptions, if $\gamma'e \leftrightarrow \gamma e$ goes back out of equilibrium at the wrong time, there is a risk that the entropy dumped into the dark photon bath from $ee \rightarrow \gamma'\gamma'$ will conflict with BBN constraints on the total radiation density. There is a competition between the heating of the γ' bath versus the heating of the visible photons during the QCD phase transition. If ϵ is very small, the freeze-out of $\gamma'e \leftrightarrow \gamma e$ occurs at such a high temperature T_f that the dark sector decouples before the QCD transition heats the visible sector, and so the dark photon temperature T_d is suppressed relative to the visible T . If ϵ is very large, the two baths remain coupled down to low temperatures, so that dark electron annihilations heat all lighter degrees of freedom equally. In this case T_d also does not exceed the visible T . Therefore we expect only a limited range of ϵ to be excluded by BBN.

We will determine the BBN constraint on ϵ in two different ways, one simpler and the other more quantitative. In the first estimate, using entropy conservation, the ratio of the dark to visible photon temperatures at the time of $\gamma'e \leftrightarrow \gamma e$ freeze-out is

$$\frac{T_d}{T} = \left[\left(\frac{2 + g_e(x_f)}{2} \right) \left(\frac{10.75}{g_*(T_f)} \right) \right]^{1/3} < 1.06 \quad (5)$$

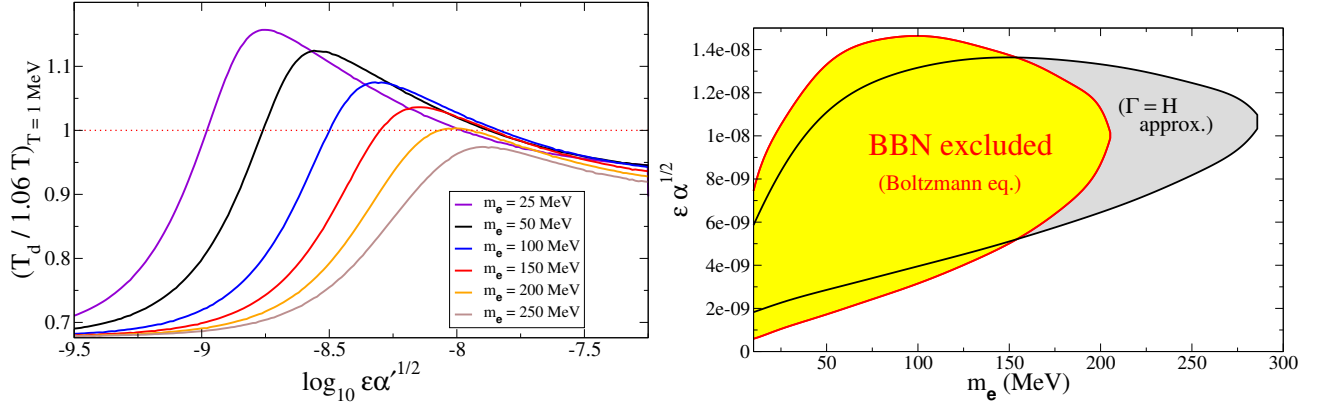


Figure 4. Left: dark to visible photon temperature ratio T_d/T at $T = 1$ MeV versus $\epsilon\sqrt{\alpha'}$, as determined by Boltzmann equations (7), for several values of the dark electron mass (curves are in order of increasing m_e from top to bottom as in legend). The minimum value of $\epsilon\sqrt{\alpha'}$ shown for a given m_e corresponds to the critical value $(\epsilon\sqrt{\alpha'})_c$ defined in the text. Right: BBN excluded regions of $\epsilon\sqrt{\alpha'}$ versus m_e for both the simple estimate based on eq. (5) and the Boltzmann code.

where $x_f = m_e/T_f$ and $g_e(x_f) \leq 3.5$ is the effective number of dark electron degrees of freedom in the plasma at the freezeout temperature T_f ,

$$g_e(x) = \frac{45}{(\pi T)^4} \int_0^\infty dp \frac{p^2(E + p^2/3E)}{e^{E/T} + 1} \quad (6)$$

while g_* is the effective number of entropy degrees of freedom in the standard model at T_f . We use the results of recent lattice studies of the QCD phase transition [84] for $g_*(T)$. In fig. 3 we show how eq. (5) depends upon T_f for a range of m_e , and the resulting excluded values of T_f versus m_e . Notably, for $m_e \gtrsim 285$ MeV, there is no constraint in this approximation, since the dark electrons annihilate early enough for their effects to be counteracted by the QCD phase transition.

By equating the $\gamma'e \leftrightarrow \gamma e$ scattering rate $\Gamma = n_e \langle \sigma v \rangle$ to the Hubble rate, we find the freeze-out temperature T_f as a function of m_e and $\alpha'\epsilon^2$. Combining this with the excluded values of T_f versus m_e , we obtain a corresponding constraint on $\epsilon\sqrt{\alpha'}$ to avoid the nucleosynthesis bound. The result is shown in fig. 4.

For a more quantitative determination of the BBN constraint, we solve the coupled Boltzmann equations for the energy densities of the dark and visible photons,

$$\begin{aligned} \frac{d\rho_{\gamma'}}{dt} &= -4H\rho_{\gamma'} + q_{\text{ann}} + q_{\text{scatt}} \\ \frac{d\rho_\gamma}{dt} &= -4H\rho_\gamma + q_{\text{SM}} - q_{\text{scatt}} \end{aligned} \quad (7)$$

where the source terms q_i are due to $ee \rightarrow \gamma'\gamma'$ annihilation, $\gamma'e \leftrightarrow \gamma e$ scattering, and $\bar{f}f \rightarrow \gamma\gamma$ annihilation of standard model particles f , respectively. Details are given in appendix A. We obtain $T_d/T = (\rho_{\gamma'}/\rho_\gamma)^{1/4}$ as a function of T in this way, and evaluate it at $T = 1$ MeV appropriate for BBN, demanding that T_d/T not exceed 1.06. The results are qualitatively similar to those of the simpler estimate, but slightly more constraining in ϵ

while less so in m_e . Fig. 4 shows that constraints exist for m_e up to 200 MeV, in contrast to the value 285 obtained previously. This limit is used, along with the relation between m_e and m_H from fixing the self-interaction cross section, to construct the BBN-excluded regions shown in fig. 2(left). We find that in general, direct detection provides a stronger constraint than BBN for this model.

II.5. Structure formation and CMB constraints

Refs. [85],[34] studied various cosmological constraints on atomic dark matter. There it is shown that the power spectrum of matter fluctuations is suppressed at small scales because of the analog of baryon acoustic oscillations, unless recombination in the dark sector occurs sufficiently early. This puts an upper bound on the interaction strength α' , but one that is easily satisfied by our models of interest for SIDM.

The main observational constraint is that the matter power spectrum should not differ from the Λ CDM prediction at scales $k < 2h\text{Mpc}^{-1}$, based on Ly- α measurements. This must be compared to the scale at which dark atom acoustic oscillations start to occur, given by the dark sector sound horizon r_d at the time of its kinetic coupling: $r_d = \int_0^{a_{\text{dec}}} c_d/(Ha^2) \cong (T_0/T_{\text{dec}})/(\sqrt{3}H_0)$, where c_d is the dark sector sound speed, which we roughly approximate as $1/\sqrt{3}$ until the time of decoupling, and zero afterwards. The kinetic decoupling temperature T_d is determined in terms of the atomic DM model parameters in [34], resulting in the lower bound

$$\frac{T_d}{E_b} > \frac{6 \times 10^{-13}}{\alpha'^6 \zeta^4} \left(\frac{E_b}{\text{keV}} \right) \left(\frac{m_H}{\text{GeV}} \right) \quad (8)$$

where E_b is the binding energy and ζ is the ratio of temperatures in the dark and visible sectors. We thus find that a sufficient condition to satisfy the Lyman- α bound

is

$$\alpha' < \frac{34}{\zeta^2} \left(\frac{m_{\mathbf{H}} \mu_{\mathbf{H}}^2}{\text{GeV}^3} \right)^{1/2} \quad (9)$$

where $\mu_{\mathbf{H}} = m_{\mathbf{H}}/f(R)$ is the dark electron reduced mass. This is satisfied for all models obeying the SIDM constraint in fig. 1.

Cosmic microwave background constraints on atomic dark matter models were summarized in ref. [32]. The main requirement is that the dark atoms be out of kinetic equilibrium with the baryon-photon plasma before recombination. This would lead to stringent constraints on the kinetic mixing parameter ϵ from Rutherford scattering if the dark atoms were ionized [86], but if the ionization fraction is negligible (as we demand) then the relevant process is Rayleigh scattering of visible photons into dark photons, which is much weaker. (The scattering of visible photons into themselves is weaker still, suppressed by a further factor of $\epsilon^2 \alpha/\alpha'$.) The cross section is given by

$$\sigma_R = \epsilon^2 \frac{\alpha}{\alpha'} \sigma_T (E_\gamma/E_b)^4 \quad (10)$$

where $\sigma_T = 8\pi\alpha^2/(3m_e^2)$ is the dark Thomson cross section and E_b is the binding energy. The rate of photon-atom interactions is $\Gamma \sim n_\gamma \sigma_R$ with $n_\gamma = 0.24 T^3$ at the recombination temperature $T_r = 0.26$ eV. Demanding that $\Gamma(T_r) < (3.8 \times 10^5 \text{y})^{-1}$, and taking $E_\gamma \cong 2.7 T_r$, we find that the constraint is satisfied by orders of magnitude even if $\epsilon \sim 1$. The same conclusion is true for the new CMB bounds on photon-dark matter scattering found by ref. [87]. We find that $\epsilon < (\alpha'/0.01)^{7/2} (m_e/\text{MeV})^{7/2}$, but m_e is $\gtrsim 0.1$ GeV for the SIDM models shown in fig. 1. Such large values of m_e imply that dark photons freeze out (via dark electron annihilation) at sufficiently high temperatures so that there is no danger of producing a too-large density of dark radiation.

Recently ref. [36] refined the constraints from dark acoustic oscillations, which could reveal the effects of dark atoms on large scale structure even in the absence of any nongravitational interaction between the two sectors. There the constraint

$$\Sigma_{\text{DAO}} = 2 \times 10^{-9} \alpha'^{-1} f(R) \left(\frac{m_{\mathbf{H}}}{1 \text{ GeV}} \right)^{-7/6} < 10^{-4} \quad (11)$$

is derived (in which we have made explicit the dependence of the binding energy on α' and the reduced mass $\mu_{\mathbf{H}}$, and used (1). Using (3) to eliminate $\alpha'^{-1} f(R)$, we find that (11) is satisfied as long as $m_{\mathbf{H}} < 10^{12}$ GeV, which has no effect on our preferred parameter space.

III. “MESONIC” DARK MATTER

Composite dark matter could be analogous to hadronic states of QCD if it is bound by a confining force associated with a nonabelian gauge symmetry. The most natural choice would be the baryonic states of such a theory,

since it is the baryons of QCD that are stable in the visible sector. However, this is not the only possibility. If there is no analog of weak or electromagnetic interactions in the dark sector, then mesonic bound states could be stable, and if lighter than the baryons, could constitute the dark matter. Glueballs of the dark sector might alternatively be the dark matter, in the case where the constituent particles are heavier than the confinement scale, or absent altogether. We consider the mesonic case in this section, and the baryonic/glueball cases in successive ones.

III.1. Elastic scattering cross section

If there are “quarks” transforming in the fundamental representation of a dark sector $\text{SU}(N)_d$, they will form mesonic $q\bar{q}$ bound states that could be stable or metastable bosonic dark matter candidates. Below the confinement scale, one expects that the elastic scattering interaction for such mesons will be strong, possibly fulfilling the criteria for SIDM. The $2 \rightarrow 2$ low-energy elastic scattering amplitude can be estimated using chiral perturbation theory (for a review, see ref. [88]), with the Lagrangian

$$\frac{F_\pi^2}{4} \text{tr} (\partial_\mu \Sigma^\dagger \partial^\mu \Sigma) + \frac{\xi}{4} F_\pi^3 \text{tr} (M \Sigma + \text{h.c.}) \quad (12)$$

where $\Sigma = e^{2i\Pi/F_\pi}$, F_π is the analog of the pion decay constant ($F_\pi = 93$ MeV for QCD), ξ is $O(1)$, and M is the dark quark mass matrix. For simplicity we take $M = m_q \mathbf{1}$, proportional to the unit matrix. If there are N_f flavors of dark quarks, then Π is a $N_f \times N_f$ matrix given by $\Pi = \pi^a T^a$, where T^a are the generators of $\text{SU}(N_f)$, normalized such that $\text{tr} T^a T^b = \frac{1}{2} \delta_{ab}$. The pion mass is given by $m_\pi^2 = \xi F_\pi m_q$.

From the $\pi\pi \rightarrow \pi\pi$ elastic scattering amplitude, we obtain the cross section (see appendix B for details)

$$\sigma = \frac{m_\pi^2}{32\pi F_\pi^4} C(N_f) \quad (13)$$

where $C(N) = (2N^4 - 25N^2 + 90 - 65/N^2)/(N^2 - 1)$. Taking for example $m_\pi \cong 1.5 F_\pi$ as in QCD, this gives $\sigma \cong 0.05 C(N_f)/m_\pi^2$. To achieve the desired SIDM cross section of $\sigma/m = 0.6 \text{ cm}^2/\text{g}$ then requires $m_\pi = (33, 36, 61, 83, 100)$ MeV for $N_f = (2, \dots, 6)$, respectively. For general choices of the ratio $x = m_\pi/F_\pi$, which depends upon the dark quark mass as $m_q^{1/2}$, these values should be rescaled by $(x/1.5)^{4/3}$. Unlike an elementary boson of such a small mass, there is no naturalness problem in principle because the mass scale is not fundamental here, but is determined by the running of the dark $\text{SU}(N)$ gauge coupling through the confinement scale $\Lambda_d \sim 4\pi F_\pi$, and the quark mass m_q whose smallness is protected by chiral symmetry.

III.2. Relic density constraints

An example providing stable “pionic” dark matter was recently proposed [67], in which the presence of two quark flavors with isospin symmetry assures the stability of the pions. In that model, nonrenormalizable interactions between the pions and the standard model were invoked so that $\pi\pi$ annihilations to SM states result in the observed relic density. These were assumed to be mediated by exchange of the Higgs or the linear combination of γ and Z corresponding to weak hypercharge, through the interactions $\lambda_h |H|^2 \text{tr}(\partial_\mu \Sigma^\dagger \partial^\mu \Sigma)$ and $\lambda_v B^{\mu\nu} \text{tr}(\Sigma^\dagger \partial_\mu \Sigma \partial_\nu \Sigma^\dagger)$ respectively.⁸ It was shown that by fixing λ_h or λ_v to give the right relic density, and imposing constraints from the invisible decays $H \rightarrow \pi\pi$ and $Z \rightarrow \pi\pi\pi$, the decay constant F_π should be greater than several times 10 GeV, which is much larger than needed for the SIDM cross section as we estimated in the previous section.

One is therefore led to question: do there exist any possible forms of interactions between the dark pions and the standard model that would allow for standard thermal production through annihilation of $\pi\pi$ into known particles, while respecting stability of the π and not conflicting with particle physics constraints? A few examples suffice to show that any mediator interactions between π and standard model fermions f , expressed as higher dimension operators such as

$$\frac{m_\pi^2 F^2}{M^4} \text{tr}(\Sigma + \Sigma^\dagger) [\bar{f} h f, \bar{f} \not{D} f, \dots] \quad (14)$$

whose strength is consistent with the desired relic density of dark pions, are suppressed by a very low scale in the denominator, $M \lesssim 1$ GeV. (If there are additional small couplings due to approximate symmetries then M must be even smaller.) Hence a thermal origin of pionic DM of such low masses requires new physics below the GeV scale coupling the dark sector to the standard model. Such models have been explored in connection with SIDM in ref. [23, 27]. Once such light mediators are admitted, the motivation to invoke compositeness to explain the strong self-interactions might be diminished, since light mediators are already sufficient for that purpose. However if the particles in the dark sector that interact with the light mediators are composite, the situation is qualitatively different from those that were previously considered. We outline such a model for light pionic DM in the next subsection.

Another possibility that admits much weaker interactions between π and the visible sector is for π to be metastable with respect to the age of the universe. For example, π could decay into light SM fermions analogously to the weak interactions, by mixing with a superheavy Z' , giving a lifetime of order $m_{Z'}^4/m_\pi^5$. For

$m_\pi \sim 100$ MeV, observations of the isotropic diffuse γ -ray background constrain the lifetime to be $\tau > 5 \times 10^{24}$ s for $\pi \rightarrow e^+e^-$ [89]. Distortions of the cosmic microwave background give a stronger limit, $\tau > 5 \times 10^{25}$ s [90], requiring $M_{Z'} \gtrsim 10^{11}$ GeV. Even if π decays only into neutrinos, the limit on $M_{Z'}$ is relaxed by a factor of just 2.6.

Given such feeble interactions, one could try to use the “freeze-in” mechanism of ref. [91] as an alternative means of thermally producing its relic abundance. By this mechanism, the relic abundance of π is predicted to be of order

$$Y_\pi \sim \frac{m_\pi^3 M_p}{M_{Z'}^4} \quad (15)$$

while the required value for the relic abundance is given by $Y_\pi = 4 \times 10^{-9} (m_\pi/100 \text{ MeV})^{-1}$. Combining this with eq. (15) gives $M_{Z'} \cong 10^6 \text{ GeV} \times (m_\pi/100 \text{ MeV})$, in strong conflict with the diffuse γ -ray or neutrino constraints. In the following we construct a model with light mediators that circumvents these constraints.

III.3. Model of light pionic DM

We can devise a model of light, strongly interacting pionic dark matter that has the desired thermal relic abundance, if the dark sector contains a broken $U(1)'$ gauge symmetry with a sufficiently light Z' gauge boson, that mixes kinetically with the photon. The model is similar to that of ref. [67], but instead of coupling the pions to the Z boson, we couple them to the Z' . If all the dark quarks have the same $U(1)'$ charge (as well as equal masses) then the diagonal (vector) $SU(N_f)$ flavor symmetry remains unbroken. The lowest dimension operator consistent with this symmetry, that couples the pions to the Z' , is

$$\frac{\lambda_0 m_q}{F_\pi} Z'_{\mu\nu} \text{tr}(\Sigma \partial^\mu \Sigma^\dagger \partial^\nu \Sigma) + \text{h.c.} \quad (16)$$

This can lead to freeze-out of the pions through the coannihilation process $\pi\pi \rightarrow \pi Z'$. However we find that the matrix element is highly velocity suppressed (d -wave, details in appendix C). The relic density is thus more likely to be determined by the higher dimension operators

$$\frac{\lambda_1}{4F_\pi^2} Z'_{\mu\nu} Z'^{\mu\nu} \text{tr}(\partial_\alpha \Sigma^\dagger \partial^\alpha \Sigma) + \frac{\lambda_2}{4F_\pi^2} Z'_{\alpha\mu} Z'^{\nu\alpha} \text{tr}(\partial^\mu \Sigma^\dagger \partial_\nu \Sigma) \quad (17)$$

that give rise to $\pi\pi \rightarrow Z'Z'$. Ignoring for simplicity the interference between these two operators, we find that the corresponding cross sections are given by

$$\sigma v = \frac{m_\pi^6}{\pi F_\pi^8} \left\{ 8\lambda_1^2, \frac{3}{2}\lambda_2^2 \right\} \quad (18)$$

⁸ The latter operator (and those in eqs. (14,16)) breaks chiral symmetry; it implicitly contains a quark mass matrix insertion

as $v \rightarrow 0$. Taking $F_\pi \cong 0.67 m_\pi \cong 24$ MeV (using the relation between F_π and m_π for QCD and the value of

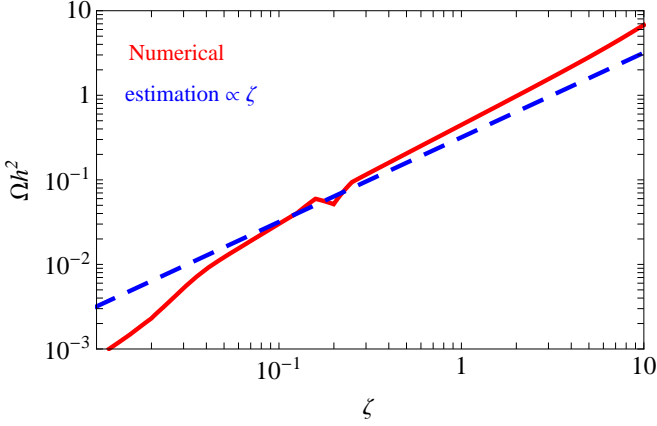


Figure 5. Dependence of relic density of pionic dark matter on ratio of hidden to visible sector temperatures, $\zeta = T_d/T_\gamma$. Dashed line shows approximate linear dependence.

m_π needed for SIDM in the case $N_f = 3$), and using the relic density cross section $\sigma v = 4.5 \times 10^{-26} \text{ cm}^3/\text{s}$ [92] appropriate for 33 MeV DM, we find that $\lambda_1 = 3 \times 10^{-7}$ or $\lambda_2 = 7 \times 10^{-7}$ to get the correct relic density.

In principle, these couplings are calculable in terms of the $U(1)'$ charge g' and masses of the dark quarks, and the confinement scale Λ of the dark $SU(N)$ gauge group. Such a calculation is difficult since it requires running down from the fundamental theory to scales below Λ . It would be interesting to know if such small values of $\lambda_{1,2}$ are consistent with reasonable choices of the parameters of the fundamental theory. In chiral perturbation theory, these couplings vanish at leading order since the pions (according to our assumption of same-charge quarks) are neutral under the $U(1)'$. Naively one expects couplings of the order $\lambda_i \sim g'^2/(16\pi^2)$ (in analogy with the anomalous vertex of π^0 to two photons in the visible sector), implying a rather small value for the coupling strength $\alpha' = g'^2/(4\pi) \sim 10^{-5}$.

The preceding calculation implicitly assumes thermal equilibrium between the dark and visible sectors, but this need not be the case. In general one expects that the dark photons (which we will argue presently should be massless) have a lower temperature T_d than the visible ones, characterized by a parameter $\zeta = T_d/T_\gamma$. In that case, $\langle\sigma v\rangle$ must be decreased by a factor $\sim \zeta$ in order to maintain the correct relic density. The modification to the Boltzmann equation in this case has been worked out in ref. [93] (see also [94]). Solving it numerically we find the dependence of the relic density on ζ shown in fig. 5. The CMB and BBN give bounds on ζ in terms of the number of the number of effective neutrino species, $\Delta N_{\text{eff}} \sim (8/7)\zeta^4$. Current bounds are roughly consistent with $\Delta N_{\text{eff}} \lesssim 1$ [95, 96], hence $\zeta \lesssim 1$. This bound is quoted in terms of the value of ζ at the time of BBN. Since photons get heated relative to dark photons afterwards, the bound on the current value of ζ is $\zeta_0 < 0.75$ [34].

III.4. CMB and charged relic constraints

In the preceding computation of the dark pion relic density, we also implicitly assumed that the dark photon temperature is not significantly increased by the dark matter annihilations themselves. If the dark sector consists only of the pions and the dark photons, having no interactions with the standard model, this will not be a valid assumption and the freezeout calculation must be revisited to take into account the heating of the dark photons. However interactions with the standard model will generically be induced via kinetic mixing $\tilde{\epsilon} F^{\mu\nu} Z'_{\mu\nu}$ between the Z' and weak hypercharge. This would help to maintain thermal equilibrium of the dark sector particles, but it also introduces a new problem by allowing the light Z' to decay into leptons and charged (visible sector) pions. This is strongly ruled out by CMB bounds since the DM is so light [97, 98].

To avoid this problem, one can take the Z' to be massless. In this case, there is no unique way of diagonalizing the gauge boson kinetic term to remove the mixing. A convenient choice is that where the field identified as the photon remains uncoupled to the dark sector, but the dark particles with $U(1)'$ charge g' acquire an electric millicharge given by $\epsilon = \tilde{\epsilon}g'/e$ [32]. In this case there is no constraint from injecting electrons into the CMB; however a fraction $\epsilon^2\alpha/\alpha'$ of annihilations will produce a visible photon. The cross section for this process is constrained as $\langle\sigma v\rangle < 1 \times 10^{-27} (m_\pi/\text{GeV}) \text{ cm}^3/\text{s}$ [99], taking into account a factor of 2 for producing only a single photon. Comparing to $\epsilon^2\alpha/\alpha'$ times the required thermal relic cross section, we obtain the bound

$$\epsilon < 1.7 \times 10^{-3} \left(\frac{\alpha'}{10^{-5}} \right)^{1/2} \left(\frac{m_\pi}{100 \text{ MeV}} \right)^{1/2} \quad (19)$$

In addition there are constraints arising from the presence of stable millicharged relics, the “baryons” of the dark sector. Unless these have a large relic abundance due to an asymmetry between particles and antiparticles, their abundance will be highly suppressed by their strong annihilation cross section. The abundance of normal baryons would be of order 10^{-19} in the absence of the baryon asymmetry [100], and even smaller in the present theory where the pion mass scale is lower and the nucleon annihilation cross section is thus larger.

The cosmological constraints on the kinetic mixing parameter of such a small population of millicharged dark baryons are weaker than the CMB bound (19). These are summarized in ref. [101], and depend upon the mass of the baryon, which in analogy to QCD we expect to be of order $7m_\pi \sim 200 - 700 \text{ MeV}$. In this mass region, ref. [101] shows that the strongest limit $\epsilon < 0.01$ comes from accelerator experiments. Stronger constraints based upon getting too large relic density do not apply to this model, since it has a large hadronic annihilation cross section not assumed in [101].

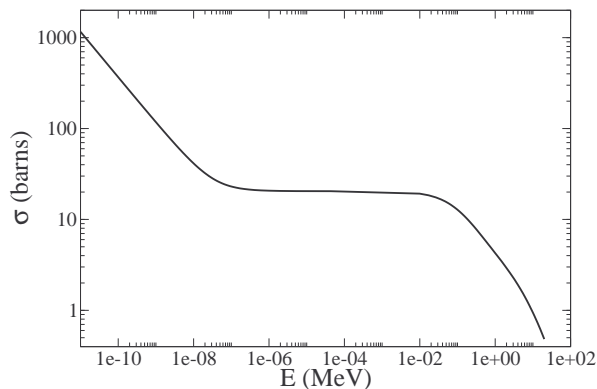


Figure 6. Isospin-averaged elastic cross section for neutron-proton scattering versus energy, using data from the ENDF library [102].

IV. DARK “BARYONS”

We turn to our next example of composite strongly interacting dark matter, in which the candidate is analogous to nucleons of the visible sector: bound states of hidden quarks confined by an unbroken $SU(N)$ gauge symmetry. For simplicity we will assume a common quark mass m_q and take the number of colors and light flavors each to be three as in QCD. The quark mass and confinement scale Λ are considered as the relevant free parameters. Equivalently, one can take the pion mass $m_\pi \sim \sqrt{m_q \Lambda}$ and Λ as the two free parameters. Also for simplicity, we will at first neglect any additional $U(1)$ interactions (dark photons) of the hidden quarks.

IV.1. SIDM constraints

As a starting point to understand the elastic scattering of dark “baryons,” we consider the example of real neutron-proton scattering, whose cross section as a function of center of mass energy is shown in fig. 6. To focus on the contribution from the strong force, we are interested in the flat region starting at energies above $E_0 \sim 0.1$ eV, since the rising cross section below this value is due to electromagnetic charge-dipole scattering. In the plateau, $\sigma \cong 20$ b, so that $\sigma/m \cong 10 \text{ cm}^2/\text{g}$, which is 17 times larger than needed for SIDM. We are interested to know how the parameters of QCD would need to be rescaled in a dark analog theory to bring this down to the desired value.

There are two parameters that primarily control the nucleon-nucleon elastic cross section. One is the confinement scale Λ of the strong $SU(N)$ interactions. Naively, one would estimate on dimensional grounds that the nucleon mass is $N_c \Lambda$ (assuming current quark masses $m_q \leq \Lambda$), while the cross-section is $\sigma \sim 4\pi \Lambda^{-2}$. Therefore $\sigma/m \sim 4\pi/(N_c \Lambda^3)$. Using this estimate and the parameters of real-world QCD, $\Lambda \sim 250$ MeV and $N_c = 3$,

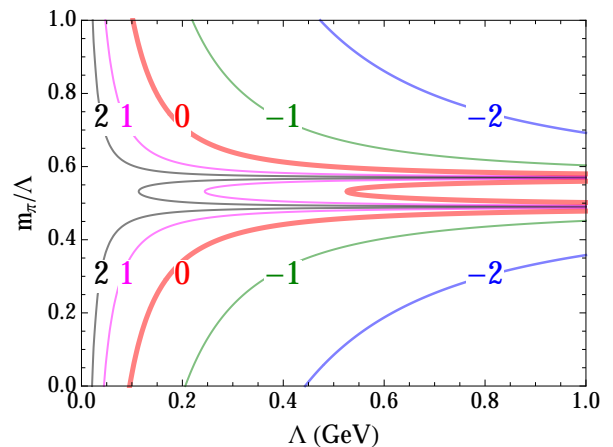


Figure 7. Contours of $\log_{10}([\sigma/m]/[0.6 \text{ cm}^2/\text{g}])$ in the plane of confinement scale Λ and pion mass m_π/Λ . Solid line (labeled “0”) corresponds to desired value.

we would estimate $\sigma/m \sim 0.2 \text{ cm}^2/\text{g}$. The naive estimate is too low by a factor of 50. The origin of the discrepancy is well-known: there is a resonant enhancement of the cross section due to the weakly bound deuteron. A better estimate for σ/m is given by $2\pi/(N_c \Lambda^2 E_b)$, where $E_b = 2.2$ MeV is the binding energy of the deuteron, which could be considered as the other parameter controlling σ .

Of course E_b is not a fundamental parameter of the theory, but it gives a clear picture of the physics controlling σ . It turns out that E_b depends sensitively on the mass of the pion (hence the quark masses). The effective range parameters for nucleon-nucleon scattering have been studied as a function of m_π in lattice gauge theory [103]. They are the scattering length a and effective range r_0 in terms of which the scattering amplitude is given by

$$\mathcal{A} = \frac{4\pi}{m_N(-ip - a^{-1} + \frac{1}{2}r_0 p^2 + O(p^4))} \quad (20)$$

where m_N is the nucleon mass and p is the center-of-mass momentum.

Fitting to the results of fig. 1 of [103], we can express the scattering lengths in the singlet and triplet spin channels as

$$a_s = \frac{0.58 \Lambda^{-1}}{m_\pi/\Lambda - 0.57}, \quad a_t = \frac{0.39 \Lambda^{-1}}{m_\pi/\Lambda - 0.49} \quad (21)$$

where we have taken $\Lambda = 250$ MeV for QCD. Here 0.49 and 0.57 are the pion-to- Λ ratios where the deuteron and the dineutron become bound; they are unbound for lighter pions and bound for heavier pions. In the analysis of [103], only m_π was varied while Λ was held fixed, but on dimensional grounds, eq. (21) should encode the right dependence if Λ were to be varied. We can therefore predict the average scattering cross section for low-velocity nucleons in a dark sector similar to QCD, but with dif-

ferent confinement scale and light quark masses,

$$\sigma = \pi(a_s^2 + 3a_t^2) \quad (22)$$

and find values of Λ and m_π in a dark analog of QCD that would give the desired value of σ/m_N , using $m_N = 3.8 \Lambda$ to agree with the visible nucleon mass.

The results are plotted in fig. 7, which shows contours of $\log_{10}([\sigma/m]/[0.6 \text{ cm}^2/\text{g}])$ as a function of Λ and m_π/Λ . The values $m_\pi/\Lambda = 0.49$ and 0.57 are where the triplet and singlet scattering lengths diverge, respectively. For $\Lambda \gtrsim 1 \text{ GeV}$, m_π/Λ needs to be close to these special values to have a large enough cross section, but for $\Lambda \lesssim 1 \text{ GeV}$, this tuning is not necessary. For $\Lambda < 100 \text{ MeV}$, large values of the pion mass $m_\pi > \Lambda$ would be required to keep the cross section sufficiently low.

We must still verify that the energies of interest for dark matter scattering coincide with the flat region of the cross section. Since we do not require dark photons in this scenario, the rising part below 0.1 eV in fig. 6 is not present in the dark analog. The fall-off after the plateau occurs when the inverse momentum of the nucleons starts to exceed the length scale $\sqrt{\sigma} \sim 3.5 a$, where in the plateau region, $a = \sqrt{\sigma/4\pi} = 13 \text{ fm}$. This corresponds to a center-of-mass energy $p^2/m_N = (4\pi a^2 m_N)^{-1} = 0.02 \text{ MeV}$, which agrees with fig. 6. For the dark baryons to be SIDM, we thus require that $(\sigma m_N)^{-1} > m_N v^2$ up to velocities $v \sim 100 \text{ km/s}$. This can be written as the constraint $m_N < (v^2 \sigma/m_N)^{-1/3} = 15 \text{ GeV}$, hence $\Lambda < 4 \text{ GeV}$ which is consistent with the parameter space plotted in fig. 7.

It has been pointed out that, if asymmetric fermionic dark matter has strong attractive interactions, their accumulation in neutron stars leads to a compact bound state that can cause gravitational collapse of the star [104, 105], yielding tighter constraints than from halo ellipticity or the Bullet Cluster. These considerations however do not apply to composite models such as the present one. Like the neutrons and protons making up neutron stars, dark nucleons are expected to exhibit short-range hard-core repulsion due to the degeneracy pressure of the underlying dark quarks, leading to an equation of state qualitatively similar to that for neutron star matter. So while attractive interactions could form a dark nucleus, the mass of dark matter required to achieve gravitational collapse should be comparable to the mass of the neutron star itself, safely more than the amount that is expected to accrete in a neutron star.

IV.2. Dark baryon relic density

Like their visible counterparts, the dark nucleons have a conserved number, and so must be asymmetric dark matter. We do not attempt to explain the origin of the asymmetry here (indeed that of the visible baryons is still unknown); it presumably arises from physics at much higher scales than that of the dark matter, which we have determined to be of order $(0.1 - 1 \text{ GeV})$. However

one may wonder why in this case the dark pions that are necessarily present have a small enough relic density. A simple possibility is that the quarks are massless so that the pions are true Goldstone bosons, and contribute only to the dark radiation density of the universe. Fig. 7 shows that $m_\pi = 0$ is compatible with $\Lambda \cong 100 \text{ MeV}$.

If the pions are massive, the existence of massless dark photons coupling to the hidden quarks would allow for them to efficiently annihilate, but this also provides a new long-range interaction between the dark nucleons, which could complicate its viability as a dark matter candidate, and require additional species to maintain the $U(1)'$ charge neutrality of the universe. A less problematic alternative would be to give the dark photons (Z') masses greater than $2m_e$, such that $\pi\pi \rightarrow Z'Z'$ annihilation would still be efficient, while $Z' \rightarrow e^+e^-$ through kinetic mixing of Z' to the photon would allow the Z' 's to decay. We consider the possibility of unstable dark pions below.

IV.3. Interactions with the standard model

An interesting consequence of coupling the dark quarks to a massive Z' is that kinetic mixing of the Z' and the photon would allow for scattering of dark baryons on protons, hence a channel for direct detection. After diagonalizing the gauge boson kinetic matrix, the proton acquires a dark millicharge $e\epsilon$; see for example [106]. Assuming the dark baryon has $U(1)'$ charge $3g'$ (taking the charge to be g' for each of three hidden sector quarks), the cross section for proton-baryon scattering is

$$\sigma_{pb} = 144\pi \alpha \alpha' \epsilon^2 \frac{\mu^2}{m_{Z'}^4}, \quad (23)$$

where $\mu = m_b m_p / (m_b + m_p)$ is the dark baryon-proton reduced mass. The resulting constraints on the kinetic mixing parameter ϵ from the LUX [76], XENON100 [79] and CDMSlite [78] experiments are shown in fig. 8.

Another possibility is to imagine heavy mediators producing isospin-violating dimension-6 couplings between the dark quarks \mathbf{q}_i (where i is the flavor index) and light standard model particles such as the electron:

$$c_{ij} \Lambda_h^{-2} (\bar{\mathbf{q}}_i \gamma_5 \gamma_\mu \mathbf{q}_j) (\bar{e} \gamma_5 \gamma^\mu e) \quad (24)$$

with c_{ij} being coefficients of order 1. We choose γ_5 couplings to match the parity of the pion; this operator allows for the decays $\pi \rightarrow e^+e^-$. By estimating the decay rate of the pion as $\Gamma_\pi = n\sigma v$ where σ is the $\mathbf{q}_i \bar{\mathbf{q}}_j \rightarrow e^+e^-$ cross section from (24), $n \sim \Lambda^3$ is the density of quarks in the pion, and $v \sim 1$, we obtain

$$\Gamma_\pi \sim \frac{m_\pi^2 \Lambda^3}{12\pi \Lambda_h^4} \quad (25)$$

To avoid overclosing the universe around the time of big bang nucleosynthesis (BBN), Γ_π should be greater than

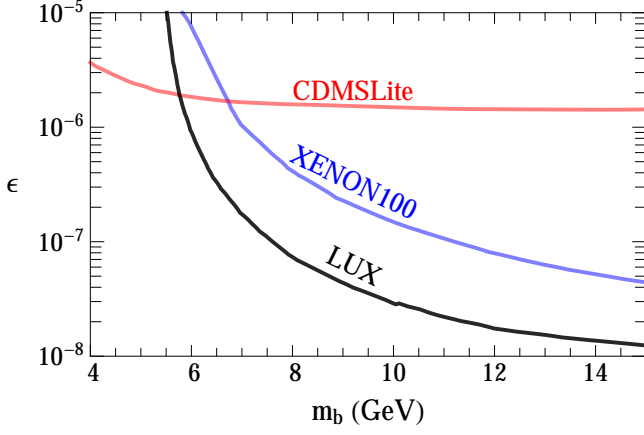


Figure 8. Constraints on kinetic mixing of massive Z' and photon from scattering of dark baryons on protons, as a function of dark baryon mass, from the LUX [76], XENON100 [79] and CDMSlite [78] experiments, assuming $g' = 1$ and $m_{Z'} = 1$ GeV. The bound on ϵ scales as $m_{Z'}^2/g'$ for other values of g' and $m_{Z'}$.

$\sim 1 \text{ s}^{-1}$. This gives an upper bound on the heavy physics scale

$$\Lambda_h < 8 \text{ TeV} \left(\frac{m_\pi}{10 \text{ MeV}} \right)^{1/2} \left(\frac{\Lambda}{100 \text{ MeV}} \right)^{3/4} \quad (26)$$

Interestingly, the same operator allows for scattering of the dark baryons from electrons. Recently the first experimental constraints on dark matter scattering from electrons were published [107], giving limits from $3 \times 10^{-38} \text{ cm}^2$ to $2 \times 10^{-37} \text{ cm}^2$ for dark matter of mass 0.1 to 1 GeV. The cross section for electron scattering with baryons containing N quarks is $\sigma_{eb} = (3N/\pi)\mu^2/\Lambda_h^4$, where $\mu \cong m_e$ is the electron-baryon reduced mass. With $N = 3$ we find the limit $\Lambda_h > 10 \text{ TeV}$. This bound starts to conflict with the need for pions to decay before big bang nucleosynthesis if m_π and Λ are near the lowest values indicated on fig. 7, as the example of $m_\pi = 10 \text{ MeV}$, $\Lambda = 100 \text{ MeV}$ shows in eq. (26).

V. DARK GLUEBALLS

If the quarks of the hidden $\text{SU}(N)$ are sufficiently heavy, then the lightest stable particle is the glueball ϕ , whose self-interaction cross section and mass can be estimated as $\sigma \sim 4\pi/\Lambda^2$, $m_\phi \sim 5.5\Lambda$. (We use the example of QCD where a likely glueball candidate has mass 1370 MeV [108] to get the factor of 5.5.) For SIDM, this leads to the requirement $\Lambda \cong 90 \text{ MeV}$, $m_\phi \cong 500 \text{ MeV}$, hence the dark quark mass should obey $m_q \gtrsim 250 \text{ MeV}$ in this scenario. Like for baryons, we expect the cross section to be velocity independent for c.m. energies $E < (\sigma m_\phi)^{-1}$. This requires $m_\phi < 15 \text{ GeV}$, which thus imposes no additional constraint.

It is challenging (perhaps impossible) to design a mediator that allows for thermal freezeout of dark glueballs by annihilation into lighter particles. Unlike pions or nucleons, whose stability could be ensured by unbroken isospin or baryon number, nothing forbids glueballs from decaying into the lighter particles once any mediator is introduced. We do not try to explain the relic density of glueballs here. It could arise from initial conditions—the relative efficiency of inflationary reheating of the visible and hidden sectors—as long as the reheating temperature was too low to bring the two sectors into equilibrium at early times.

V.1. CMB constraint versus direct detection

Nevertheless there are some generic statements that can be made about the nature of mediators between dark glueballs and the standard model. Suppose that new particles at the high scale Λ_h induce an effective interaction between the dark gluon (with field strength $G_{\mu\nu}$) and standard model gauge singlet operators \mathcal{O}_{sm} of dimension n :

$$\frac{1}{\Lambda_h^n} G_{\mu\nu} G^{\mu\nu} \mathcal{O}_{\text{sm}} \quad (27)$$

We assume that the gluon operator G^2 interpolates between ϕ and the vacuum as $\langle 0|G^2|\phi \rangle \sim (m_\phi \Lambda)^{3/2}$; this parametrization agrees with the $\Gamma \sim n\sigma v$ estimate used previously for pion decays, with $n \sim \Lambda^3$. Thus (27) leads to decays of ϕ if \mathcal{O}_{sm} consists of states that are lighter than m_ϕ , such as γ, e, μ . Such decays are subject to stringent CMB constraints; for example the lifetime for $\phi \rightarrow e^+e^-$ for 500 MeV dark matter must satisfy $\tau > 4 \times 10^{24} \text{ s} \cong 10^{49} \text{ GeV}^{-1}$ [90]. Assuming that $\langle e\bar{e}|\mathcal{O}_{\text{sm}}|0 \rangle \sim m_e m_\phi^{n-3}$ (since the operator is chirality-suppressed and the electrons have energy of order m_ϕ), we find the decay rate $\Gamma_\phi \sim (m_\phi/16\pi)(\Lambda/m_\phi)^3(m_e/m_\phi)^2(m_\phi/\Lambda_h)^{2n}$, hence the constraint

$$\left(\frac{\Lambda_h}{m_\phi} \right)^n \gtrsim 10^{19} \quad (28)$$

taking $m_\phi = 5.5\Lambda = 0.5 \text{ GeV}$. For a 4-body decay such as $\phi \rightarrow e^+e^-e^+e^-$ this would be increased by $(m_\phi/m_e)/(4\pi^2) \sim 10^{3/2}$ since it need no longer be chirality suppressed, but does suffer from a phase space reduction $\sim (4\pi^2)^9$.

The same interactions that cause 2-body glueball decays give rise to elastic scattering with visible matter, because the GG operator also interpolates between the vacuum and the two-glueball state, with $\langle 0|GG|\phi\phi \rangle \sim m_\phi^2$.

⁹ The ratio of phase spaces for the 4- and 2-body rates is of order $(m_\phi^2/4\pi^2)^2$. We have extracted the factors of m_ϕ to make the dimensionless ratio in (28) and taken the square root since (28) is a bound on the amplitude.

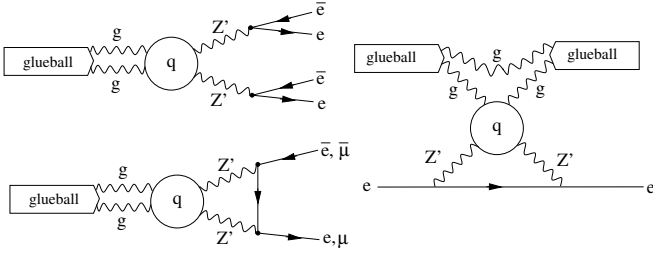


Figure 9. Upper left: decay of dark glueball into $e^+e^-e^+e^-$ by virtual Z' emission through dark quark loop. Lower left: related decays into e^+e^- , or $\mu^+\mu^-$, which is subdominant if $m_q < 8$ GeV. Right: leading contribution to dark glueball-electron scattering, which is shown to be negligible.

(For this part of the argument, the distinction between m_ϕ and Λ is not important.) The cross section for $\phi e \rightarrow \phi e$ from (27) is therefore of order

$$\sigma_{\phi e} \sim m_\phi^{-2} \left(\frac{m_\phi}{\Lambda_h} \right)^{2n} \lesssim 10^{-66} \text{ cm}^2 \quad (29)$$

using (28). This is many orders of magnitude below the current limit discussed below eq. (26). We see that the CMB bound on ϕ decays is so strong that crossing symmetry implies that its scattering interactions are necessarily negligible.

In passing we observe that a similar argument shows that one cannot get a large enough annihilation cross section of glueballs for them to have the right thermal relic density if their lifetime is greater than that of the universe. Consider for example the coupling of glueballs to light Z' gauge bosons through the operator $\Lambda_h^{-4} \text{tr}(G_{\mu\nu} G^{\mu\nu}) Z'_{\alpha\beta} Z'^{\alpha\beta}$, which gives rise to both decays $\phi \rightarrow Z'Z'$ and annihilations $\phi\phi \rightarrow Z'Z'$. Demanding that the lifetime exceed 10^{18} s gives a cross section less than 10^{-66} cm^2 .

V.2. Heavy Z' mediator between glueball and SM

As a concrete example, we consider as mediator a heavy Z' gauge boson that couples to the hidden quarks and to leptons with strength α' . Integrating out the hidden quarks and Z' s leads to several possible operators giving glueball decay, including $\mathcal{O}_1 = (\bar{e}\gamma^\mu e)^2$ and $\mathcal{O}_2 = \bar{\mu}\mu$. (We will presently see that the operator $\bar{e}e$ gives rise to a much smaller contribution to the decay width, hence we focus on muons for \mathcal{O}_2 .) Fig. 9 shows the corresponding diagrams for decays into $e^+e^-e^+e^-$ and $\mu^+\mu^-$. The first one has heavy scale given by $\Lambda_1^{-6} \sim 64\pi\alpha_N\alpha'^2 m_\phi^2 / (360 m_q^4 m_{Z'}^4)$ where $\alpha_N = g_N^2/4\pi$ is the hidden SU(N) gauge coupling.¹⁰ The second operator is chirality- and loop-suppressed and has $\Lambda_2^{-3} \sim$

$m_\mu\alpha_N\alpha'^2/(16\pi m_{Z'}^4)$. Taking into account the phase space ratio $\sim (m_\phi^2/4\pi^2)^2$, the 2-body and 4-body decay rates become comparable for $m_q \cong 0.7$ GeV. This is somewhat larger than the minimum dark quark mass of $m_\phi/2 \sim 0.25$ GeV needed to ensure that the glueball is lighter than the meson. The CMB constraint (28) then leads to the bound

$$m_{Z'} \gtrsim 2.3 \text{ TeV} \left(\frac{\alpha_N\alpha'^2}{10^{-5}} \right)^{1/4} \begin{cases} x^{-1}, & x < 1 \\ 1, & x > 1 \end{cases} \quad (30)$$

where $x = m_q/(0.7 \text{ GeV})$. The strong coupling α_N should be evaluated at the scale m_q , hence $\alpha_N \sim 1$ if m_q is near the confinement scale, but smaller otherwise.

This shows that the new physics can be at a relatively low scale accessible at LHC, despite the large ratio in (28). For a Z' with couplings $\alpha' \sim 0.003$ to ordinary quarks (the “sequential standard model”, SSM), ATLAS obtains the limit $m_{Z'} \gtrsim 3 \text{ TeV}$ [109] from resonant dilepton searches. Thus it is possible that a mediator between the standard model and metastable glueball dark matter, consistent with CMB constraints on the glueball decays, could be discovered at the LHC.

To extract limits from the ATLAS results, we computed the expected number of dilepton events in the model with coupling $\sqrt{4\pi\alpha'} Z'_\mu \bar{f}\gamma^\mu f$ to all SM fermions and dark quarks, but ignoring the contribution of Z' decays into dark quarks to compute branching ratio B to leptons. (This is justified if the number of dark quarks is small compared to the number of SM fermions). Comparing to the limit on σB of ref. [109], we obtain the constraint as a function of Z' mass

$$\log_{10} \alpha' < -5.71 + 0.410 y + 0.267 y^2 \quad (31)$$

where $y = m_{Z'}$ in TeV. To compare this with the CMB bound we treat (31) as an equality to eliminate α' in (30), and assume $\alpha_N \sim 1$, resulting in a lower bound on m_q as a function of $m_{Z'}$ shown in fig. 10. This is the CMB bound on models that are discoverable in the next run of the LHC. The range of allowed quark masses is mostly consistent with our requirement that glueballs be lighter than mesons in the dark sector for this scenario (indicated by the dashed line), while still being relatively small. The implication is that models on the verge of discovery through Z' production at the LHC could also

¹⁰ The quark loop in the 4-body decay diagram generates an Euler-Heisenberg-like effective interaction between the gluons and the Z' field strength, $\alpha_N\alpha'/(360 m_q^4)[\text{tr}(G^2)Z'^2 + 7 \text{tr}(G\tilde{G})Z\tilde{Z}]$. The factor of 64π comes from $g'^2 = 4\pi\alpha'$, the coefficients $1 + 7 = 8$, each Z' field strength containing two vector fields, and the Z' momenta going as $p_1 \cdot p_2 \sim m_\phi^2/2$. To estimate the second decay diagram, it is easiest to first do the loop containing the Z' s, which is dominated by momenta of order $m_{Z'}$ and requires mass insertions of the SM fermion and the dark quark. This loop is of order $g'^4 m_\mu m_q / (16\pi^2 m_{Z'}^4)$. The quark loop, dominated by momenta of order m_q , now has only three propagators, requiring one more mass insertion, and so contributes $\sim g_N^2 m_q / (4 \cdot 16\pi^2 m_q^2)$ to the $G_{\mu\nu}G^{\mu\nu}$ effective operator.

¹⁰ The quark loop in the 4-body decay diagram generates an Euler-Heisenberg-like effective interaction between the gluons and the

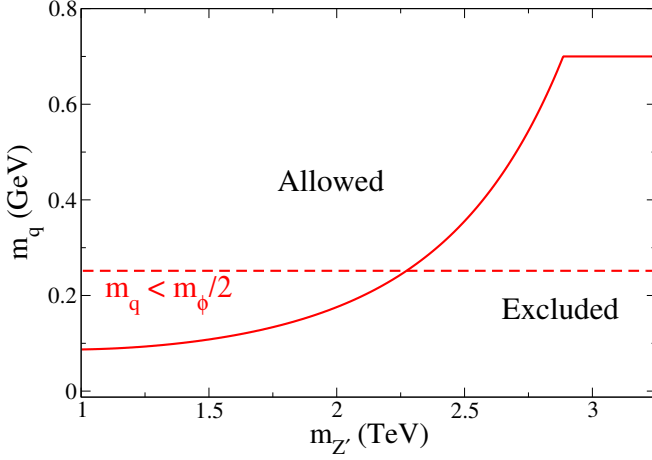


Figure 10. Lower bound from CMB on dark quark mass m_q as a function of $m_{Z'}$, for couplings α' that saturate the ATLAS constraint from dileptonic decays of Z' [109]. Below the dashed line is theoretically disfavored since glueballs would be heavier than mesons in that region.

be close to having an impact on the CMB for reasonable choices of parameters. Such a Z' might also reveal the number of dark quark species through the measurement of its invisible width.

V.3. Higgs portal mediation

As a second example, we imagine that the heavy particles are scalars S in the fundamental representation of the hidden $SU(N)$, that communicate with the standard model through the Higgs portal interaction $\lambda|S|^2|H|^2$. Integrating out the scalar gives the SM operator $\mathcal{O} = |H|^2$ with $\Lambda_h^{-2} = \lambda\alpha_N/m_S^2$. The Higgs boson mediates the decay $\phi \rightarrow \bar{\mu}\mu$, with rate

$$\Gamma_\phi \sim \frac{m_\mu^2(m_\phi\Lambda)^3 m_\phi}{16\pi\Lambda_h^4 m_h^4} \quad (32)$$

Demanding that $\Gamma < 10^{-49}$ GeV as before, we obtain the bound

$$m_S > 10^7 \text{ GeV} \left(\frac{\lambda\alpha_N}{0.01} \right)^{1/2} \quad (33)$$

which is inaccessible to the LHC. The bound is much stronger in this case than for the Z' mediator because the matrix element is suppressed by only $1/m_S^2$; compare to $1/m_{Z'}^4$ in the previous model.

V.4. Neutrino portal mediation

Since the CMB constraints are so severe, one might ask whether dark glueballs could have larger interactions with the SM if they decayed only into neutrinos

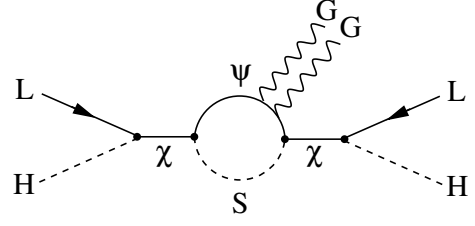


Figure 11. Diagram to generate neutrino portal interaction $(LH)^2$ coupling to the dark glueball operator $G_{\mu\nu}G^{\mu\nu}$.

rather than charged leptons. However the constraints from Super-Kamiokande on DM decay into neutrinos are still quite strong [89]: for decay of a 500 MeV glueball, the lifetime must exceed 2×10^{22} s, which is only 100 times weaker than the CMB bound on leptonic decays. To illustrate, we consider an example in which the SM operator coupling to $G_{\mu\nu}G^{\mu\nu}$ is the neutrino portal [110] $(LH)^2$ where L is a charged lepton doublet. Then the effective operator is

$$\mathcal{O} = \Lambda_h^{-5} (LH)^2 G^2 = \Lambda_h'^{-3} \bar{\nu}\nu GG \quad (34)$$

In the second form, we absorb the Higgs VEVs v^2 into Λ_h^{-5} to display the relevant form of the operator at energies below the weak scale. The decay rate is then $\Gamma \sim (\Lambda m_\phi)^3 m_\phi / 16\pi \Lambda_h'^6$ and we obtain the bound $\Lambda_h' > 5600$ TeV.

As a concrete example, a model that can generate the desired interaction was presented in ref. [61], where the dark sector contains a scalar S and fermion ψ in the fundamental representation (here however we take their electric charges to vanish) and a singlet fermion χ , with Yukawa interactions $y_\chi \bar{\chi} S^* \psi$ and $y_\nu \bar{\chi} H L$. The $(LH)^2 G_{\mu\nu}G^{\mu\nu}$ effective operator is generated by the diagram shown in fig. 11, with coefficient $\Lambda_h^{-5} = (y_\chi^2 y_\nu^2 / 16\pi^2) m_\chi^{-2} m_S^{-3}$ where we take $m_S \sim m_\psi = m_{S/\psi}$. There is also a seesaw contribution to the neutrino masses of order $(y_\nu v)^2 / m_\chi$, which must be $\lesssim 0.2$ eV. Regardless of that or other details of the theory however, the main point is that scattering of the glueballs with visible matter, mediated by the same diagram as in fig. 11 (but with gluon lines associated to different glueballs as in fig. 9, right), is suppressed by the same large factor of $\Lambda_h'^6$ as in the decay rate. The neutrino portal thus offers no substantial relaxation of the scale by which interactions of the glueballs with the visible sector must be suppressed.

VI. SUMMARY AND CONCLUSIONS

The possibility that dark matter self-scatters elastically with a velocity-independent cross section $\sigma \sim 1\text{b} \times (m/\text{GeV})$ is motivated by the cusp/core and too-big-to-fail problems of structure formation with cold dark matter. These problems may find alternative solutions, as

we mentioned in section I; in that case the quoted cross section is at least still allowed by current constraints. In previous literature, the possibility to get such a large cross section from light mediators was explored. Here we have investigated for this purpose various forms of composite dark matter, that can naturally have strong self-interactions. We examined the cases where dark matter is analogous to atoms, molecules, mesons, baryons, or glueballs.

Atomic dark matter bound by a new $U(1)'$ interaction was found to be viable as a SIDM candidate for a large range of values of the ratio $R = m_p/m_e$ (the dark proton to electron masses), with $U(1)'$ coupling $\alpha' \gtrsim 0.03$ and mass $m_H \sim 0.3(R/\alpha')^{2/3}$ GeV (this follows from the rough estimate $\sigma \sim 100a_0^2$ of the cross section). The same estimate is also valid if the atoms are primarily bound into H_2 molecules. In both cases, the dark coupling should satisfy $\alpha' \gtrsim 0.03$ to avoid a significant fraction of ionized constituents. The question of whether dark atoms will exist mostly within molecules is interesting but beyond the scope of the present paper. However the absence of dark stars (hence ionizing dark radiation) suggests that molecules will be prevalent. See ref. [37] for a more detailed discussion. Another interesting feature of dark atoms is that the cross-section typically has non-trivial velocity dependence at the low velocities relevant to cosmology, generally being larger at lower velocities relevant in dwarf galaxies than at higher velocities relevant in clusters.

In the case of dark mesons, bound by an $SU(N)$ interaction with confinement scale Λ , a low mass $m_\pi \sim 30 - 100$ MeV is required for them to be SIDM, depending upon the number of hidden quark flavors and the ratio $m_q/\Lambda \sim m_\pi^2/\Lambda^2$. We found that dark pions in this mass range can have a thermal origin if there is a very weakly coupled ($\alpha' \sim 10^{-5}$) massless $U(1)'$ in the hidden sector that kinetically mixes with the photon. In this case the hidden quarks acquire electric millicharges ϵe . As long as the dark baryons (which are also millicharged) have no asymmetry, their relic abundance is very small and the constraint on ϵ from charged relics is weak, $\epsilon \lesssim 2 \times 10^{-3}$. A comparable and more secure bound $\epsilon \lesssim 2 \times 10^{-3}$ arises from CMB constraints on annihilations into visible plus dark photons.

If the dark matter is in the form of nucleon-like bound states, it can be SIDM with masses typically in the range $m_B \sim 0.1 - 1$ GeV. Larger values are possible if the dark pion mass happens to be close to where one of the scattering lengths diverges, $m_\pi \cong 0.49\Lambda$ or 0.57Λ , suggested by lattice studies. We determined the relations between Λ and m_π that give the desired SIDM cross section in QCD-like dark sectors. To avoid overclosure of the universe by the dark pions, they should either be massless or else unstable. The latter case implies interactions with the standard model that can lead to direct detection.

Dark glueballs, whose mass should be ~ 500 MeV in order to be SIDM, are generally more problematic than the other candidates in terms of having the right relic

density and additional direct or indirect detection signatures. Their couplings to the standard model are tightly constrained by their effect on the CMB through decays. These interactions are thus shown to be too weak to mediate direct detection. However, they can be consistent with mediators at the TeV scale that could be discovered at the LHC, as we showed in an explicit example with a Z' mediator. A low reheat temperature after inflation would be needed to prevent a thermal population of glueballs, which would overclose the universe.

Apart from glueballs, all of the candidates we have considered are motivated (through relic density considerations) to have significant interactions with the standard model, including couplings to a dark photon, either massless or massive, that can mix with the visible photon. This gives the possibility for direct or indirect signals that could provide additional observational probes of the models. In the case of dark atoms, the kinetic mixing parameter ϵ is already strongly constrained by the XENON100 bound, as shown in fig. 2. A prediction of our dark meson model is the existence of a very small population of millicharged dark baryons that might be discovered in more sensitive searches for anomalous isotopes. Conversely if dark baryons dominate, then the same interactions that would deplete dark mesons through decays can generate scattering of the baryons on electrons at a level that is already constrained using XENON10 data.

We expect future simulations of structure formation and astrophysical studies [111]-[114] to improve our understanding of whether strong self-interactions of dark matter are really needed, or to what extent they are allowed. If such interactions arise from the composite nature of dark matter, our study shows that its mass should be $\sim 10 - 100$ GeV if it is in atomic/molecular form, or $\sim 0.1 - 1$ GeV if it is mesonic/baryonic. In either case, there are several independent observables that could provide complementary tests.

Acknowledgments. We thank Carlos Frenk, Annika Peter, Francis-Yan Cyr-Racine, Kris-Sigurdson, Sean Tulin, Alfredo Urbano and Jure Zupan for helpful discussions. JC thanks the Aspen Center for Physics for providing a stimulating working environment while this research was in progress.

Appendix A: BBN constraint on dark photons

In this appendix we provide details of our implementation of the BBN bound on the dark photon temperature. In both the approximate and more exact methods, we make use of the thermally averaged cross section for mixed Compton scattering on dark electrons, $\gamma'e \leftrightarrow \gamma e$. In the rest frame of the initial e , the cross section is given by $\sigma(w) = \sigma_T f(w)$ where w depends upon the initial photon energy E_i as $w \equiv E_i/m_e$ and [115] (see eq.

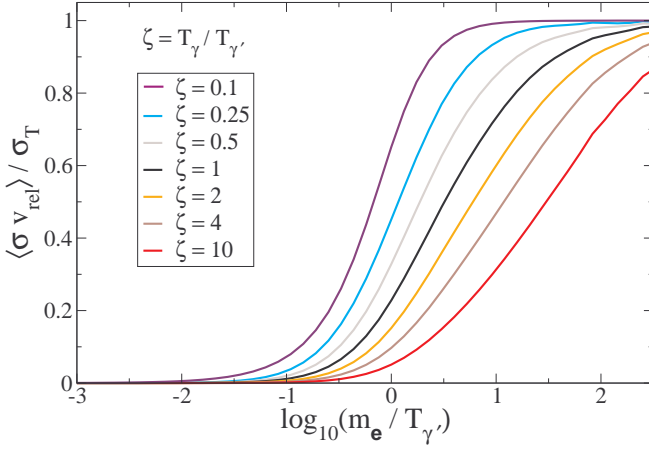


Figure 12. Thermally averaged cross section for $\gamma e \rightarrow \gamma' e$ at several values of $\zeta = T_{\gamma}/T_{\gamma'} \equiv T/T_d$, in order of increasing ζ from top to bottom. The dependence upon ζ only applies for $\gamma e \rightarrow \gamma' e$, not the reverse process, which corresponds to $\zeta = 1$.

(5-116))

$$f(w) = \frac{3}{4} \left\{ \frac{1+w}{w^3} \left[\frac{2w(1+w)}{1+2w} - \ln(1+2w) \right] + \frac{\ln(1+2w)}{2w} - \frac{1+3w}{(1+2w)^2} \right\} \quad (\text{A1})$$

The Thomson cross section is given by $\sigma_T = (8\pi/3)\alpha\alpha'(\epsilon/m_e)^2$. For the thermal average, we take

$$\langle \sigma v \rangle_{\gamma \rightarrow \gamma'} = \int \frac{d^3 p_e}{(2\pi)^3} \int \frac{d^3 p_{\gamma'}}{(2\pi)^3} f_{\gamma} f_e \sigma(w) |\vec{v}_{\text{rel}}| \quad (\text{A2})$$

where $w = \frac{1}{2}(s/m_e^2 - 1)$ in terms of the Mandelstam invariant $s = (E_e + E_{\gamma})^2 - (\vec{p}_e + \vec{p}_{\gamma})^2$ and $\vec{v}_{\text{rel}} = \vec{p}_e/E_e - \vec{p}_{\gamma}/E_{\gamma}$. For the process $\gamma e \rightarrow \gamma' e$, we allow for different temperatures in the two sectors, so that the (normalized) distribution functions have the dependences $f_{\gamma} = f_{\gamma}(p_{\gamma}, T_{\gamma})$, $f_e = f_e(p_e, T_d)$. In contrast, for $\gamma' e \rightarrow \gamma e$, we take both initial particles to have temperature $T_d = T_{\gamma'}$, since we assume that $\gamma' e \leftrightarrow \gamma' e$ scattering is strong enough to keep the dark particles in kinetic equilibrium for as long as there is a significant e population. Carrying out the thermal average in (A2) numerically, we obtain the results shown in fig. 12 for a range of visible to dark temperature ratios, $\zeta = T/T_d$. We find that $\langle \sigma v \rangle / \sigma_T$ can be approximated by the analytic form

$$\frac{\langle \sigma v \rangle}{\sigma_T} \cong \left(\frac{1}{2} (1 + \tanh(A_0 \log_{10} x - A_1)) \right)^{A_2} \quad (\text{A3})$$

where $x = m_e/T_d$ and the coefficients A_i depend upon ζ as shown in table I. We can thus rapidly interpolate between the ζ values of interest without having to repeat the integration in (A2).

For the simplified approach in which we estimate the freezeout temperature T_f via $\Gamma = n_e \langle \sigma v \rangle = H$, we take

ζ	A_0	A_1	A_2
0.1	2.209	0.041	0.583
0.25	1.420	-0.0056	1.156
0.5	1.099	-0.092	1.843
1	0.934	-0.037	2.265
2	0.854	0.189	2.112
4	0.817	0.496	1.773
10	0.786	0.878	1.496

Table I. Coefficients for the analytic fit (A3) to the thermally averaged $\gamma' e \leftrightarrow \gamma e$ scattering cross section.

$\zeta = 1$. In the more quantitative Boltzmann analysis, the distinction enters into the source term q_{scatt} which we take to be

$$q_{\text{scatt}} = n_e (\langle \sigma v \rangle_{\gamma \rightarrow \gamma'} \rho_{\gamma} - \langle \sigma v \rangle_{\gamma' \rightarrow \gamma} \rho_{\gamma'}) \quad (\text{A4})$$

where ρ_i are the energy densities. The cross section $\langle \sigma v \rangle_{\gamma \rightarrow \gamma'}$ depends upon ζ whereas $\langle \sigma v \rangle_{\gamma' \rightarrow \gamma}$ depends only upon the dark photon temperature through m_e/T_d (and corresponds to the case $\zeta = 1$). When q_{scatt} is large compared to $H\rho_i$, it drives the two photon baths toward equilibrium with each other.

The other source terms in the Boltzmann equations are given by

$$q_{\text{SM}} = \frac{4}{3} H \frac{\rho_{\gamma} \frac{d \ln g_*}{d \ln T_{\gamma}}}{1 + \frac{1}{3} \frac{d \ln g_*}{d \ln T_{\gamma}}} \quad (\text{A5})$$

$$q_{\text{ann}} = \frac{4}{3} H \frac{\rho_{\gamma'} \frac{d \ln g_d}{d \ln T_d}}{1 + \frac{1}{3} \frac{d \ln g_d}{d \ln T_d}} \quad (\text{A6})$$

where $g_d = 2 + g_e$ is the effective number of degrees of freedom in the dark plasma. These are a straightforward consequence of entropy conservation as the photons get heated by annihilation of heavier standard model particles, or the dark photons are heated by dark electron annihilation. For reference we display $g_*(T)$ in fig. 13(left). It is found by adding the contributions from photons and leptons to the QCD degrees of freedom determined by ref. [84]. The dependence of $d \ln g_d / d \ln T_d$ on $x = m_e/T_d$ is shown in fig. 13(right).

Appendix B: Pion scattering at low energy

In this appendix we provide details of the elastic cross section for dark pion scattering at low energy, derived from the chiral Lagrangian (12). Expanding to fourth order in the pion field Π , the relevant interaction terms are

$$\mathcal{L}_{4\pi} = \frac{1}{3F_{\pi}^2} \text{tr} \left[\left(\Pi \overset{\leftrightarrow}{\partial}^{\mu} \Pi \right) \left(\Pi \overset{\leftrightarrow}{\partial}_{\mu} \Pi \right) + m_{\pi}^2 \Pi^4 \right] \quad (\text{B1})$$

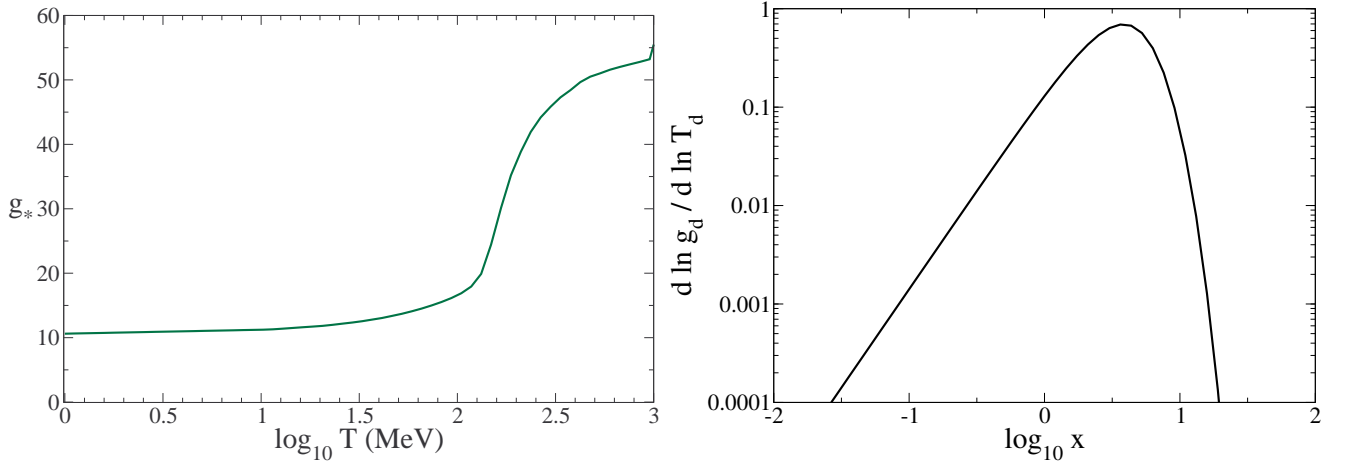


Figure 13. Left: Effective number of degrees of freedom g_* versus temperature, inferred from ref. [84]. Right: Dependence of $d \ln g_d / d \ln T_d$ on $x = m_e / T_d$, appearing in the source term q_{ann} .

The matrix element of the process $\pi^a + \pi^b \rightarrow \pi^c + \pi^d$ derived from B1) is

$$\begin{aligned}
 -i\mathcal{M} = & (\text{tr} [T^a T^b T^c T^d] + (b \leftrightarrow d)) \frac{2(2m_\pi^2 - t)}{F_\pi^2} + \\
 & (\text{tr} [T^a T^c T^b T^d] + (c \leftrightarrow d)) \frac{2(2m_\pi^2 - s)}{F_\pi^2} + \\
 & (\text{tr} [T^a T^c T^d T^b] + (b \leftrightarrow c)) \frac{2(2m_\pi^2 - u)}{F_\pi^2}
 \end{aligned} \quad (\text{B2})$$

In the case of SU(2), $\text{tr}[T^a T^b T^c T^d] = \frac{1}{8} (\delta_{ab}\delta_{cd} + \delta_{ad}\delta_{bc} - \delta_{ac}\delta_{bd})$ [116, 117]. For general SU(N),

$$\text{tr}[T^a T^b T^c T^d] = \frac{1}{4N} \delta_{ab}\delta_{cd} + \frac{1}{8} (d^{abe} + i f^{abe}) (d^{cde} + i f^{cde}) \quad (\text{B3})$$

and the isospin-averaged matrix element squared (using Mathematica) is

$$\begin{aligned}
 |\mathcal{M}|^2 &= \frac{1}{(N^2 - 1)^2} \sum_{abcd} |\mathcal{M}_{abcd}|^2 \\
 &= \frac{[8(2N^4 - 25N^2 + 90 - 65N^{-2}) m_\pi^4 - (3N^4 - 37N^2 + 132 - 96N^{-2}) (s t + t u + u s)]}{2F_\pi^4 (N^2 - 1)}
 \end{aligned} \quad (\text{B4})$$

Therefore, the cross section at center-of-mass momentum p is

$$\sigma_{2\pi \rightarrow 2\pi} = \frac{[(2N^4 - 25N^2 + 90 - 65N^{-2}) m_\pi^4 + 2(3N^4 - 37N^2 + 132 - 96N^{-2}) (m_\pi^2 p^2 - \frac{5}{6} p^4)]}{32\pi F_\pi^4 (N^2 - 1)(m_\pi^2 + p^2)} \quad (\text{B5})$$

Appendix C: Pion coannihilation to a light gauge boson

The interaction (16) does not respect the full $\text{SU}(3)_L \times \text{SU}(3)_R$ chiral flavor symmetry $\Sigma \rightarrow V^\dagger \Sigma U$, but it does respect the diagonal subgroup $\Sigma \rightarrow V^\dagger \Sigma V$, requiring the quark mass insertion that we have made explicit. (The quark mass matrix takes the place of the missing Σ^\dagger field.) Expanding (16) to leading order in the pion

fields gives

$$-4 \frac{\lambda_0 m_q}{F_\pi^4} Z'_{\mu\nu} f_{abc} \pi^a \partial^\mu \pi^b \partial^\nu \pi^c \quad (\text{C1})$$

Defining $\tilde{\lambda} = 4\lambda_0 m_q / F_\pi^4$, the matrix element for the process $\pi^a(p_1) + \pi^b(p_2) \rightarrow \pi^c(p_3) + Z'(p_4)$ is (up to a phase)

$$2\tilde{\lambda} (\epsilon^\mu p_4^\nu - \epsilon^\nu p_4^\mu) f_{abc} [p_2^\mu p_3^\nu - p_1^\mu p_3^\nu - p_1^\mu p_2^\nu] \quad (\text{C2})$$

where ϵ^μ is the polarization vector of Z' . The isospin-averaged, squared matrix element is given by

$$\begin{aligned} \langle |\mathcal{M}|^2 \rangle &= -\frac{9\tilde{\lambda}^2 N_f}{4(N_f^2 - 1)} (st(s+t) - 3m_\pi^2 st + m_\pi^6) \\ &\cong \frac{135\tilde{\lambda}^2 N_f}{4(N_f^2 - 1)} m_\pi^6 v^4 \end{aligned} \quad (\text{C3})$$

where the second line gives the low-energy limit, with v being the velocity of the incoming particles in the c.m. frame.

-
- [1] A. Borriello and P. Salucci, *Mon. Not. Roy. Astron. Soc.* **323**, 285 (2001) [astro-ph/0001082].
 - [2] F. Donato, G. Gentile, P. Salucci, C. F. Martins, M. I. Wilkinson, G. Gilmore, E. K. Grebel and A. Koch *et al.*, *Mon. Not. Roy. Astron. Soc.* **397**, 1169 (2009) [arXiv:0904.4054 [astro-ph.CO]].
 - [3] W. J. G. de Blok, *Adv. Astron.* **2010**, 789293 (2010) [arXiv:0910.3538 [astro-ph.CO]].
 - [4] W. J. G. de Blok and A. Bosma, *Astron. Astrophys.* **385**, 816 (2002) [astro-ph/0201276].
 - [5] M. Boylan-Kolchin, J. S. Bullock and M. Kaplinghat, *Mon. Not. Roy. Astron. Soc.* **415**, L40 (2011) [arXiv:1103.0007 [astro-ph.CO]].
 - [6] M. Boylan-Kolchin, J. S. Bullock and M. Kaplinghat, *Mon. Not. Roy. Astron. Soc.* **422**, 1203 (2012) [arXiv:1111.2048 [astro-ph.CO]].
 - [7] D. N. Spergel and P. J. Steinhardt, *Phys. Rev. Lett.* **84**, 3760 (2000) [astro-ph/9909386].
 - [8] R. Davé, D. N. Spergel, P. J. Steinhardt and B. D. Wandelt, *Astrophys. J.* **547**, 574 (2001) [astro-ph/0006218].
 - [9] D. H. Weinberg, J. S. Bullock, F. Governato, R. K. de Naray and A. H. G. Peter, arXiv:1306.0913 [astro-ph.CO].
 - [10] E. Polisensky and M. Ricotti, *Mon. Not. Roy. Astron. Soc.* **437**, 2922 (2014) [arXiv:1310.0430 [astro-ph.CO]].
 - [11] J. Miralda-Escude, *Ap. J.* **564** (2002) 60 [astro-ph/0002050].
 - [12] S. W. Randall *et al.*, *Astrophys. J.* **679**, 1173 (2008) [arXiv:0704.0261 [astro-ph]].
 - [13] A. H. G. Peter, M. Rocha, J. S. Bullock and M. Kaplinghat, arXiv:1208.3026 [astro-ph.CO].
 - [14] M. Rocha, A. H. G. Peter, J. S. Bullock, M. Kaplinghat, S. Garrison-Kimmel, J. Onorbe and L. A. Moustakas, *Mon. Not. Roy. Astron. Soc.* **430**, 81 (2013) [arXiv:1208.3025 [astro-ph.CO]].
 - [15] J. Zavala, M. Vogelsberger and M. G. Walker, *Monthly Notices of the Royal Astronomical Society: Letters* **431**, L20 (2013) [arXiv:1211.6426 [astro-ph.CO]].
 - [16] M. G. Walker and J. Penarrubia, *Astrophys. J.* **742**, 20 (2011) [arXiv:1108.2404 [astro-ph.CO]].
 - [17] L. E. Strigari, C. S. Frenk and S. D. M. White, *Mon. Not. Roy. Astron. Soc.* **408**, 2364 (2010) [arXiv:1003.4268 [astro-ph.CO]].
 - [18] J. L. Feng, M. Kaplinghat and H. -B. Yu, *Phys. Rev. Lett.* **104**, 151301 (2010) [arXiv:0911.0422 [hep-ph]].
 - [19] M. R. Buckley and P. J. Fox, *Phys. Rev. D* **81**, 083522 (2010) [arXiv:0911.3898 [hep-ph]].
 - [20] A. Loeb and N. Weiner, *Phys. Rev. Lett.* **106**, 171302 (2011) [arXiv:1011.6374 [astro-ph.CO]].
 - [21] M. Vogelsberger, J. Zavala and A. Loeb, *Mon. Not. Roy. Astron. Soc.* **423**, 3740 (2012) [arXiv:1201.5892 [astro-ph.CO]].
 - [22] L. G. van den Aarssen, T. Bringmann and C. Pfrommer, *Phys. Rev. Lett.* **109**, 231301 (2012) [arXiv:1205.5809 [astro-ph.CO]].
 - [23] S. Tulin, H. -B. Yu and K. M. Zurek, *Phys. Rev. D* **87**, no. 11, 115007 (2013) [arXiv:1302.3898 [hep-ph]].
 - [24] L. Pearce and A. Kusenko, *Phys. Rev. D* **87**, 123531 (2013) [arXiv:1303.7294 [hep-ph]].
 - [25] R. Laha, B. Dasgupta and J. F. Beacom, *Phys. Rev. D* **89**, 093025 (2014) [arXiv:1304.3460 [hep-ph]].
 - [26] B. Bellazzini, M. Cliche and P. Tanedo, *Phys. Rev. D* **88**, no. 8, 083506 (2013) [arXiv:1307.1129].
 - [27] M. Kaplinghat, S. Tulin and H. -B. Yu, arXiv:1308.0618 [hep-ph].
 - [28] L. Ackerman, M. R. Buckley, S. M. Carroll and M. Kamionkowski, *Phys. Rev. D* **79**, 023519 (2009) [arXiv:0810.5126 [hep-ph]].
 - [29] D. E. Kaplan, G. Z. Krnjaic, K. R. Rehermann and C. M. Wells, *JCAP* **1005**, 021 (2010) [arXiv:0909.0753 [hep-ph]].
 - [30] S. R. Behbahani, M. Jankowiak, T. Rube and J. G. Wacker, *Adv. High Energy Phys.* **2011**, 709492 (2011) [arXiv:1009.3523 [hep-ph]].
 - [31] D. E. Kaplan, G. Z. Krnjaic, K. R. Rehermann and C. M. Wells, *JCAP* **1110**, 011 (2011) [arXiv:1105.2073 [hep-ph]].
 - [32] J. M. Cline, Z. Liu and W. Xue, *Phys. Rev. D* **85**, 101302 (2012) [arXiv:1201.4858 [hep-ph]].
 - [33] J. M. Cline, Z. Liu and W. Xue, *Phys. Rev. D* **87**, 015001 (2013) [arXiv:1207.3039 [hep-ph]].
 - [34] F. -Y. Cyr-Racine and K. Sigurdson, *Phys. Rev. D* **87**, 103515 (2013) [arXiv:1209.5752 [astro-ph.CO]].
 - [35] J. Fan, A. Katz, L. Randall and M. Reece, *Phys. Dark Univ.* **2**, 139 (2013) [arXiv:1303.1521 [astro-ph.CO]].
 - [36] F. -Y. Cyr-Racine, R. de Putter, A. Raccanelli and K. Sigurdson, *Phys. Rev. D* **89**, 063517 (2014) [arXiv:1310.3278 [astro-ph.CO]].
 - [37] J. M. Cline, Z. Liu, G. Moore and W. Xue, *Phys. Rev. D* **89**, 043514 (2014) [arXiv:1311.6468 [hep-ph]].
 - [38] M.Y. Khlopov, *Mod. Phys. Lett. A* **26**, 2823 (2011) [arXiv:1111.2838 [astro-ph.CO]].
 - [39] K. Jedamzik and M. Pospelov, *New J. Phys.* **11**, 105028 (2009) [arXiv:0906.2087 [hep-ph]].

- [40] M. Pospelov, private communication
- [41] T. Yamagata, Y. Takamori and H. Utsunomiya, Phys. Rev. D **47**, 1231 (1993).
- [42] R. Laha and E. Braaten, Phys. Rev. D **89**, 103510 (2014) [arXiv:1311.6386 [hep-ph]].
- [43] Z. Berezhiani, Int. J. Mod. Phys. A **19**, 3775 (2004) [hep-ph/0312335].
- [44] R. Foot, Int. J. Mod. Phys. D **13**, 2161 (2004) [astro-ph/0407623].
- [45] Z. Berezhiani, Eur. Phys. J. ST **163**, 271 (2008).
- [46] A. E. Faraggi and M. Pospelov, Astropart. Phys. **16**, 451 (2002) [hep-ph/0008223].
- [47] K. Hamaguchi, S. Shirai and T. T. Yanagida, Phys. Lett. B **654**, 110 (2007) [arXiv:0707.2463 [hep-ph]].
- [48] T. Hur, D. -W. Jung, P. Ko and J. Y. Lee, Phys. Lett. B **696**, 262 (2011) [arXiv:0709.1218 [hep-ph]].
- [49] J. L. Diaz-Cruz, Phys. Rev. Lett. **100**, 221802 (2008) [arXiv:0711.0488 [hep-ph]].
- [50] K. Hamaguchi, E. Nakamura, S. Shirai and T. T. Yanagida, Phys. Lett. B **674**, 299 (2009) [arXiv:0811.0737 [hep-ph]]; JHEP **1004**, 119 (2010) [arXiv:0912.1683 [hep-ph]].
- [51] D. S. M. Alves, S. R. Behbahani, P. Schuster and J. G. Wacker, Phys. Lett. B **692**, 323 (2010) [arXiv:0903.3945 [hep-ph]].
- [52] G. D. Kribs, T. S. Roy, J. Terning and K. M. Zurek, Phys. Rev. D **81**, 095001 (2010) [arXiv:0909.2034 [hep-ph]].
- [53] M. Lisanti and J. G. Wacker, Phys. Rev. D **82**, 055023 (2010) [arXiv:0911.4483 [hep-ph]].
- [54] R. Barbieri, S. Rychkov and R. Torre, Phys. Lett. B **688**, 212 (2010) [arXiv:1001.3149 [hep-ph]].
- [55] D. Spier Moreira Alves, S. R. Behbahani, P. Schuster and J. G. Wacker, JHEP **1006**, 113 (2010) [arXiv:1003.4729 [hep-ph]].
- [56] M. Blennow, B. Dasgupta, E. Fernandez-Martinez and N. Rius, JHEP **1103**, 014 (2011) [arXiv:1009.3159 [hep-ph]].
- [57] T. Hur and P. Ko, Phys. Rev. Lett. **106**, 141802 (2011) [arXiv:1103.2571 [hep-ph]].
- [58] E. Del Nobile, C. Kouvaris and F. Sannino, Phys. Rev. D **84**, 027301 (2011) [arXiv:1105.5431 [hep-ph]].
- [59] K. Kumar, A. Menon and T. M. P. Tait, JHEP **1202**, 131 (2012) [arXiv:1111.2336 [hep-ph]].
- [60] M. Frigerio, A. Pomarol, F. Riva and A. Urbano, JHEP **1207**, 015 (2012) [arXiv:1204.2808 [hep-ph]].
- [61] J. M. Cline, A. R. Frey and G. D. Moore, Phys. Rev. D **86**, 115013 (2012) [arXiv:1208.2685 [hep-ph]].
- [62] M. R. Buckley and E. T. Neil, Phys. Rev. D **87**, 043510 (2013) [arXiv:1209.6054 [hep-ph]].
- [63] T. Higaki, K. S. Jeong and F. Takahashi, JCAP **1308**, 031 (2013) [arXiv:1302.2516 [hep-ph]].
- [64] M. Heikinheimo, A. Racioppi, M. Raidal, C. Spethmann and K. Tuominen, Mod. Phys. Lett. A **29**, 1450077 (2014) [arXiv:1304.7006 [hep-ph]].
- [65] C. Kouvaris, Phys. Rev. D **88**, no. 1, 015001 (2013) [arXiv:1304.7476 [hep-ph]].
- [66] Y. Bai and P. Schwaller, Phys. Rev. D **89**, 063522 (2014) [arXiv:1306.4676 [hep-ph]].
- [67] S. Bhattacharya, B. Melic and J. Wudka, JHEP **1402**, 115 (2014) [arXiv:1307.2647].
- [68] M. Holthausen, J. Kubo, K. S. Lim and M. Lindner, JHEP **1312**, 076 (2013) [arXiv:1310.4423 [hep-ph]].
- [69] R. Bernabei *et al.* [DAMA and LIBRA Collaborations], Eur. Phys. J. C **67**, 39 (2010) [arXiv:1002.1028 [astro-ph.GA]].
- [70] P. L. Biermann, H. J. de Vega and N. G. Sanchez, arXiv:1305.7452 [astro-ph.CO].
- [71] D. J. E. Marsh and J. Silk, MNRAS, Volume 437, p2652 (2013) [arXiv:1307.1705 [astro-ph.CO]].
- [72] U. Seljak, A. Makarov, P. McDonald and H. Trac, Phys. Rev. Lett. **97**, 191303 (2006) [astro-ph/0602430].
- [73] M. Viel, G. D. Becker, J. S. Bolton, M. G. Haehnelt, M. Rauch and W. L. W. Sargent, Phys. Rev. Lett. **100**, 041304 (2008) [arXiv:0709.0131 [astro-ph]].
- [74] A. Schneider, D. Anderhalden, A. Maccio and J. Die-mand, arXiv:1309.5960 [astro-ph.CO].
- [75] R. Kennedy, C. Frenk, S. Cole and A. Benson, arXiv:1310.7739 [astro-ph.CO].
- [76] D. S. Akerib *et al.* [LUX Collaboration], Phys. Rev. Lett. **112**, 091303 (2014) [arXiv:1310.8214 [astro-ph.CO]].
- [77] C. E. Aalseth *et al.* [CoGeNT Collaboration], Phys. Rev. Lett. **106**, 131301 (2011) [arXiv:1002.4703 [astro-ph.CO]].
- [78] R. Agnese *et al.* [SuperCDMSSoudan Collaboration], Phys. Rev. Lett. **112**, 041302 (2014) [arXiv:1309.3259 [physics.ins-det]].
- [79] E. Aprile *et al.* [XENON100 Collaboration], Phys. Rev. Lett. **109**, 181301 (2012) [arXiv:1207.5988 [astro-ph.CO]].
- [80] S. Yellin, Phys. Rev. D **66**, 032005 (2002) [physics/0203002].
- [81] E. D. Carlson and S. L. Glashow, Phys. Lett. B **193**, 168 (1987).
- [82] Z. Berezhiani and A. Lepidi, Phys. Lett. B **681**, 276 (2009) [arXiv:0810.1317 [hep-ph]].
- [83] R. H. Cyburt, B. D. Fields, K. A. Olive and E. Skillman, Astropart. Phys. **23**, 313 (2005) [astro-ph/0408033].
- [84] S. Borsanyi, G. Endrodi, Z. Fodor, A. Jakovac, S. D. Katz, S. Krieg, C. Ratti and K. K. Szabo, JHEP **1011**, 077 (2010) [arXiv:1007.2580 [hep-lat]].
- [85] J. L. Feng, M. Kaplinghat, H. Tu and H. -B. Yu, JCAP **0907**, 004 (2009) [arXiv:0905.3039 [hep-ph]].
- [86] S. D. McDermott, H. -B. Yu and K. M. Zurek, Phys. Rev. D **83**, 063509 (2011) [arXiv:1011.2907 [hep-ph]].
- [87] R. J. Wilkinson, J. Lesgourgues and C. Boehm, JCAP **1404**, 026 (2014) [arXiv:1309.7588 [astro-ph.CO]].
- [88] H. Georgi, "Weak Interactions and Modern Particle Theory," Menlo Park, Usa: Benjamin/cummings (1984) 165p
- [89] N. F. Bell, A. J. Galea and K. Petraki, Phys. Rev. D **82**, 023514 (2010) [arXiv:1004.1008 [astro-ph.HE]].
- [90] R. Diamanti, L. Lopez-Honorez, O. Mena, S. Palomares-Ruiz and A. C. Vincent, JCAP **1402**, 017 (2014) [arXiv:1308.2578 [astro-ph.CO]].
- [91] L. J. Hall, K. Jedamzik, J. March-Russell and S. M. West, JHEP **1003**, 080 (2010) [arXiv:0911.1120 [hep-ph]].
- [92] G. Steigman, B. Dasgupta and J. F. Beacom, Phys. Rev. D **86**, 023506 (2012) [arXiv:1204.3622 [hep-ph]].
- [93] J. L. Feng, H. Tu and H. -B. Yu, JCAP **0810**, 043 (2008) [arXiv:0808.2318 [hep-ph]].
- [94] S. Das and K. Sigurdson, Phys. Rev. D **85**, 063510 (2012) [arXiv:1012.4458 [astro-ph.CO]].
- [95] G. Steigman, Adv. High Energy Phys. **2012**, 268321 (2012) [arXiv:1208.0032 [hep-ph]].

- [96] P. A. R. Ade *et al.* [Planck Collaboration], arXiv:1303.5076 [astro-ph.CO].
- [97] D. P. Finkbeiner, S. Galli, T. Lin and T. R. Slatyer, Phys. Rev. D **85**, 043522 (2012) [arXiv:1109.6322 [astro-ph.CO]].
- [98] J. M. Cline and P. Scott, JCAP **1303**, 044 (2013) [Erratum-ibid. **1305**, E01 (2013)] [arXiv:1301.5908 [astro-ph.CO]].
- [99] L. Lopez-Honorez, O. Mena, S. Palomares-Ruiz and A. C. Vincent, JCAP **1307**, 046 (2013) [arXiv:1303.5094 [astro-ph.CO]].
- [100] E. W. Kolb and M. S. Turner, Front. Phys. **69**, 1 (1990).
- [101] S. Davidson, S. Hannestad and G. Raffelt, JHEP **0005**, 003 (2000) [hep-ph/0001179].
- [102] Evaluated Nuclear Data File (ENDF) library, <http://www-nds.iaea.org/exfor/endl.htm>
- [103] J. -W. Chen, T. -K. Lee, C. -P. Liu and Y. -S. Liu, Phys. Rev. C **86**, 054001 (2012) [arXiv:1012.0453 [nucl-th]].
- [104] C. Kouvaris, Phys. Rev. Lett. **108**, 191301 (2012) [arXiv:1111.4364 [astro-ph.CO]].
- [105] J. Bramante, K. Fukushima, J. Kumar and E. Stopnitzky, Phys. Rev. D **89**, 015010 (2014) [arXiv:1310.3509 [hep-ph]].
- [106] F. Chen, J. M. Cline and A. R. Frey, Phys. Rev. D **80**, 083516 (2009) [arXiv:0907.4746 [hep-ph]].
- [107] R. Essig, A. Manalaysay, J. Mardon, P. Sorensen and T. Volansky, Phys. Rev. Lett. **109**, 021301 (2012) [arXiv:1206.2644 [astro-ph.CO]].
- [108] W. Ochs, J. Phys. G **40**, 043001 (2013) [arXiv:1301.5183 [hep-ph]].
- [109] [ATLAS Collaboration], ATLAS-CONF-2013-017.
- [110] A. Falkowski, J. Juknevič and J. Shelton, arXiv:0908.1790 [hep-ph].
- [111] C. J. Saxton, arXiv:1212.5294 [astro-ph.CO].
- [112] F. Kahlhoefer, K. Schmidt-Hoberg, M. T. Frandsen and S. Sarkar, Mon. Not. Roy. Astron. Soc. **437**, 2865 (2014) [arXiv:1308.3419 [astro-ph.CO]].
- [113] D. Harvey, E. Tittley, R. Massey, T. D. Kitching, A. Taylor, S. R. Pike, S. T. Kay and E. T. Lau *et al.*, arXiv:1310.1731 [astro-ph.CO].
- [114] A. N. Baushev, arXiv:1312.0314 [astro-ph.CO].
- [115] C. Itzykson and J. B. Zuber, New York, Usa: Mcgraw-hill (1980) 705 P.(International Series In Pure and Applied Physics)
- [116] S. Weinberg, Phys. Rev. Lett. **17**, 616 (1966).
- [117] S. Scherer, Adv. Nucl. Phys. **27**, 277 (2003) [hep-ph/0210398].